Journal of Computational Physics **151,** 881–909 (1999)
Article ID jcph.1999.6225, available online at http://www.idealibrary.com on IDEAL®

Mimetic Discretizations for Maxwell's Equations

James M. Hyman and Mikhail Shashkov

Los Alamos National Laboratory, T-7, MS-B284, Los Alamos, New Mexico 87545
E-mail: jh@lanl.gov, misha@+7.lanl.gov

Received September 28, 1998; revised February 3, 1999

We have constructed reliable finite difference methods for approximating the solution to Maxwell's equations using accurate discrete analogs of differential operators that satisfy the identities and theorems of vector and tensor calculus in discrete form. The numerical approximation does not have spurious modes and mimics many fundamental properties of the underlying physical problem including conservation laws, symmetries in the solution, and the nondivergence of particular vector fields. Numerical examples demonstrate the high quality of the method when the medium is strongly discontinuous and for nonorthogonal, nonsmooth computational grids.

Key Words: Maxwell's equations; mimetic finite difference methods; discrete vector analysis; numerical methods.

1. INTRODUCTION

We will construct conservative finite difference methods (FDMs) for two-dimensional Maxwell's curl equations for multimaterial medium on nonorthogonal, nonsmooth, logically rectangular computational grid. These FDMs are based on the discrete analogs of first-order differential operators, **div**, **grad**, and **curl**, that satisfy discrete analogs of the theorems of vector analysis. The new methods produce solutions free of spurious modes and satisfy the divergence-free conditions exactly. The properties of the discrete operators guarantee the stability of the FDMs and allow powerful iterative methods to solve the systems of linear equations relating to these FDMs.

This paper is a part of our attempt to develop a discrete analog of vector and tensor calculus that can be used to accurately approximate continuum models for a wide range of physical processes on logically rectangular, nonorthogonal, nonsmooth grids. These *mimetic* FDMs *mimic* fundamental properties of the original continuum differential operators and allow the discrete approximations of partial differential equations (PDEs) to preserve critical properties including conservation laws and symmetries in the solution of the underlying physical problem. In particular, we have constructed discrete analogs of first-order differential

0021-9991/99

operators, such as **div**, **grad**, and **curl**, that satisfy the discrete analogs of theorems of vector and tensor calculus [10–13]. This approach has also been used to construct high-quality mimetic FDMs for the divergence and gradient in approximating the diffusion equation [15, 38, 39].

In this paper we apply our new methodology to construct mimetic FDMs to Maxwell's first-order curl equations,

$$\frac{\partial \vec{B}}{\partial t} = -\mathbf{curl}\,\vec{E}, \qquad \frac{\partial \vec{E}}{\partial t} = \frac{1}{\epsilon}\,\mathbf{curl}\,\frac{\vec{B}}{\mu}, \tag{1.1}$$

where $\vec{B}$ is the magnetic flux density and $\vec{E}$ is the electric field intensity. The permittivity, ϵ, and permeability, μ, can be general symmetric positive-definite tensors with possibly discontinuous elements at the interface between different media. We chose this form for the equations because at the interface between two media the normal components of $\vec{B}$ and the tangential components of $\vec{E}$ are continuous (see, for example, [32]). This approach is consistent with the discrete operators described in [10–13], that also uses these vectors components.

In addition to Eqs. (1.1), the following "divergence-free" conditions

$$\mathbf{div}\,\vec{D} = 0, \qquad \mathbf{div}\,\vec{B} = 0, \tag{1.2}$$

are satisfied. Here $\vec{D} = \epsilon\vec{E}$ is the electric flux density. If the solution of (1.1) satisfies these "divergence-free" conditions initially, then they will be satisfied at later times [32]. Because we use discrete operators that satisfy discrete analogs of theorems of vector analysis, the discrete analogs of "divergence-free" conditions are automatically a consequence of the discrete "curl" equations.

In this paper we consider 2-D logically rectangular grids, where the tensors determining material properties are defined in the grid cells, and assume that the interface between different materials coincides with the faces of the cells. We describe the primary variable $\vec{E}$ by its orthogonal projection onto the directions of edges of the computational cells and the primary variable $\vec{B}$ is described by its orthogonal projection onto the directions normal to the cell faces.

Because we use different discrete descriptions of the magnetic and electric fields we need two different discrete analogs of **curl**. To discretize $\mathbf{curl}\,\vec{E}$ we use a coordinate invariant definition of the $\mathbf{curl}\,\vec{E}$ based on Stokes' circulation theorem applied to the faces of the cell. This definition defines the discrete analog of Faraday's law of electromagnetic induction locally for each face.

When discretizing the second equation in (1.1), when ϵ and μ are discontinuous and (or) the computational grid is not smooth, then it is not possible to separate the discretization of $\mathbf{curl}\,\vec{B}$ from the discretization of $\frac{1}{\epsilon}\,\mathbf{curl}\,\frac{\vec{B}}{\mu}$. We construct a discrete analog of the full operator $\frac{1}{\epsilon}\,\mathbf{curl}\,\frac{\vec{B}}{\mu}$ using a discrete analog of the integral identity for curls

$$\int_V (\vec{A}, \mathbf{curl}\,\vec{B})\,dV - \int_V (\vec{B}, \mathbf{curl}\,\vec{A})\,dV = \oint_{\partial V} ([\vec{B}\times\vec{A}], \vec{n})\,dS, \tag{1.3}$$

which is also responsible for the law of conservation of electromagnetic energy. Here $\vec{A}$ and $\vec{B}$ are arbitrary vector functions, and $(\cdot,\cdot)$ and $[\cdot\times\cdot]$ are dot and cross product of two vectors,

respectively, and $\vec{n}$ is the unit outward normal to the surface ∂V of volume V. This approach guarantees that the electromagnetic energy is conserved on the discrete level. This construction is done within the framework of the support-operators method (SOM) [33, 35, 38].

To discretize the condition $\mathbf{div}\,\vec{B}=0$ we use the natural coordinate invariant definition of the divergence based on Gauss' divergence theorem. It is shown in [10] that this discrete divergence satisfies the discrete analog of identity $\mathbf{div}\,\mathbf{curl}\,\vec{E}=0$ in each cell. Therefore if a discrete analog of $\mathbf{div}\,\vec{B}=0$ holds initially, then it will hold for later times.

To discretize the condition $\mathbf{div}\,\vec{D}=\mathbf{div}\,\epsilon\vec{E}=0$, we must define a discrete analog of operator $\mathbf{div}\,\epsilon\cdot$. Following the approach used in [11], we construct a discrete $\mathbf{div}\,\epsilon$ operator using the integral identity

$$\int_V (\vec{W}, \mathbf{grad}\,u)\,dV = -\int_V u\,\mathbf{div}\,\vec{W}\,dV + \oint_{\partial V} u(\vec{W},\vec{n})\,dS, \tag{1.4}$$

where $\vec{W}$ and u are arbitrary vector and scalar functions, and the natural discretization of the **grad** operator is based on its connection to the directional derivative. We prove that these operators satisfy a discrete analog of the identity $\mathbf{div}\,\mathbf{curl}\,\vec{H}=0$. Therefore if the discrete analog of $\mathbf{div}\,\epsilon\vec{E}=0$ holds initially, then it will hold for later times.

Using these discrete spatial operators, which we denote using capital letters (CURL $\sim$ **curl** and ${}_\epsilon\overline{\mathrm{CURL}}_\mu \sim \frac{1}{\epsilon}\,\mathbf{curl}\,\frac{\cdot}{\mu}$), we consider the following discretization of Maxwell's curl equations

$$\frac{\vec{B}_h^{n+1}-\vec{B}_h^{n}}{\Delta t} = -\mathrm{CURL}\,\vec{E}_h^{\alpha_1}, \qquad \frac{\vec{E}_h^{n+1}-\vec{E}_h^{n}}{\Delta t} = {}_\epsilon\overline{\mathrm{CURL}}_\mu\,\vec{B}_h^{\alpha_2}, \tag{1.5}$$

where $\vec{E}_h^{\alpha_1}=\alpha_1\vec{E}_h^{n+1}+(1-\alpha_1)\vec{E}_h^{n}$ and $\vec{B}_h^{\alpha_2}=\alpha_2\vec{B}_h^{n+1}+(1-\alpha_2)\vec{B}_h^{n}$, and $t_n=\Delta t n$. For some problems with strongly discontinuous coefficients, it is important to preserve energy. It is easy to show that the only method of this form which preserves energy is the midpoint method ($\alpha_1=\alpha_2=0.5$). To solve the system of linear equations arising when using this implicit scheme we reduce the original discrete system of equations to a system of equations, which contains only the unknown $\vec{E}_h^{n+1}$. The adjointness property of the discrete curls guarantees that the resulting system of equations will be symmetric and positive-define (SPD). After solving for $\vec{E}_h^{n+1}$, the first equation in (1.5) is used to explictly definite $\vec{B}_h^{n+1}$.

These discrete operators also can be used to discretize the equations of magnetic diffusion [41]

$$\frac{\partial\vec{B}}{\partial t} = -\mathbf{curl}\,\vec{E}, \qquad \sigma\vec{E} = \mathbf{curl}\,\frac{\vec{B}}{\mu},$$

which arise in magnetohydrodynamics (MHD) [14]. Here the conductivity σ is a symmetric positive-definite discontinuous tensor. The equations of magnetic diffusion are often solved together with Lagrangian hydrodynamics. The Lagrangian grids move with the media and can be extremely distorted or rough; FDMs have to be robust and accurate on these grids. The numerical examples presented in Section 8 and [14] demonstrate that our FDM is accurate on nonsmooth grids.

Implicit time integration methods are required to efficiently solve these equations in many practical applications. When integrating the equations with an implicit method our approach guarantees that the system of linear equations is SPD even on highly distorted grids. The SPD property allows powerful interative methods to be used to solve these equations.

The remainder of this paper is organized as follows. In Section 2 we give a brief overview of methods for solving Maxwell's equations. In Section 3 we dicuss the properties of the governing equations preserved by the discrete model. In Section 4 we describe the grid, the discretizations of scalar and vector functions, and the inner products in the discrete function spaces. In Section 5 we review the derivation of the natural and adjoint finite difference analogs for the divergence, gradient, and curl and introduce discrete analogs of the operators $\mathbf{div}\,\epsilon\cdot$ and $\frac{1}{\epsilon}\,\mathbf{curl}\,\frac{\cdot}{\mu}$. We also define the discrete analogs of the theorems of vector analysis needed for the derivations in this paper. In Section 6 we describe our FDMs and prove that they satisfy the desired properties. In Section 7 we discuss the solution of implicit equations. Finally in Section 8, we present the numerical examples.

2. BACKGROUND

There is a huge literature related to solving Maxwell's equations. We want to note that our method on *orthogonal grids* is identical to the finite-difference time-domain (FDTD) method developed by Yee [44] and the structure of discrete operators is the same as in the MAFIA family of methods, [43].

Recently Yee's method has been extended for general grids (see, for example, [42, pp. 369–374] and references therein). These generalizations use the original grid and a newly defined dual grid. Faraday's law is discretized on the original grid and the electric field, $\vec{E}$, is defined by components on the edges of the grid, which can be interpreted as the flow of the electric field along the cell edges. This description agrees with the method we are proposing if our components for $\vec{E}$ are multiplied by the length of the edges. The magnetic flux, $\vec{B}$, is described in these methods by the components on the cell faces. These components can be interpreted as the flux through the face of the cell, and agree with components we are using up to a factor of face area. Ampere's law is discretized on the dual grid using the same procedure (with respect to edges and faces of the dual grid) for the magnetic field, $\vec{H}$, and the electric flux, $\vec{D}$. The discretizations of the equations in terms of these variables are straightforward.

However, to close the system the discrete analogs of constitutive equations $\vec{D}=\epsilon\vec{E}$ and $\vec{B}=\mu\vec{H}$ must be defined consistent with the discretization. Because $\vec{D}$ and $\vec{E}$ (as well as $\vec{B}$ and $\vec{H}$) are defined in different locations, it is not trivial to define a consistent interpolation procedure, when coefficients are discontinuous and the grid is nonsmooth. Most procedures use the connection between the co- and contravariant components of the vector to construct the interpolation formula. The potential disadvantages of this approach are clear when we consider nonsmooth grids and the case of discontinuous coefficients.

There are several possible approaches to define the dual grid. For example, in [42] the dual grid formed by connecting the centers of the cells of the original grid is adequate for the smooth grid but is a poor choice if the grid is nonsmooth. On very irregular grids the edges of this dual grid may fail to intersect the corresponding face of the original grid and instead intersect faces of other cells, or even cross several cells. When this happens, and μ and ϵ are discontinuous and the interfaces coincide with faces of the original grid, then the interpolation formulas for the constitutive equations are unlikely to even be consistent. That is, the naive interpolation can lead to errors which do not vanish as grid size goes to zero (see [39, pp. 402–404]), lead to stability problems [34], and introduce spurious modes into the solution [16].

It is recognized [34] that FDMs will be stable if interpolation operators are symmetric and positive-definite. These properties can be achieved for reasonably regular grids by manipulation of the local basis vectors related to original and the dual grids [34]. This framework can be used to interpret our approach as a consistent way to define symmetric positive-definite interpolation operators (material matrices, using terminology from [43, 34]) without using the dual grids.

The FDM and analysis is presented here for the first time for general problems. However, for the equations of magnetic diffusion Shashkov and others published a series of papers (independent of Yee's paper) constructing variational FDMs on logically rectangular grids [19]. For this particular problem the discretization and location of variables are the same as the method we are proposing. The discretizations of the curl operator constructed in these papers have been applied to the solutions of Maxwell's equations in cylindrical geometry on orthogonal grids [7] and to modeling a microwave plasma generator [21]. The stability and convergence of the variational FDMs have been theoretically analyzed [2], using the energy method based on the adjointness property of the discrete operators.

Algebraic topology provides a natural framework to describe discrete structures. The ideas of algebraic topology have been applied to developing numerical methods (especially on rectangular grids) for more than 40 years (see references in [10]). By applying this approach to electromagnetics (see, for example, [3] and references therein) formal structures can be introduced that correspond to the objects of electromagnetics. The "edge elements" and "facet elements" introduced in this approach correspond to our discretization of the electric and magnetic fields. The main difficulties in this approach are the construction of consistent adjoint operators or using terminology of algebraic topology, discrete analogs of the Hodge operator. This paper and [10–13] provide a self-consistent derivation of FDMs based on the discrete vector analysis without resorting to the terminology or machinery of algebraic topology.

There is continuing discussion about the origin of spurious solutions that arise in computational electromagnetic models (e.g., [16, 17] and references there). Spurious solutions for FDMs for first-order systems can originate from inconsistent discretizations of the operators **div**, **curl**, and **grad**. SOM FDMs defined in a consistent way are free of spurious solutions. The consistent definition of the initial electric and magnetic fields can be achieved using the discrete analogs of the orthogonal decomposition theorem proved in [12]. That is, given discrete divergence and curl of a discrete vector, the full vector can be uniquely reconstructed and decomposed into two orthogonal vectors in a unique way, satisfying a discrete analog of the formula $\vec{A} = \mathbf{grad}\,\varphi + \mathbf{curl}\,\vec{B}$, if its normal or tangential component is given on the boundary.

A discrete vector field theory on Delaunay–Voronoi meshes is created in [28, 29]. This theory uses the special geometrical property of the Delaunay–Voronoi meshes that the sides of Delaunay triangulation are orthogonal to the corresponding sides of the Voronoi polygons. The local orthogonality property makes these grids similar to the usual orthogonal grids. Another important property of these grids is that vertices of triangles can be also considered as "centers" of the Voronoi cells. This approach leads to a natural generalization of the standard staggered mesh FDM for Maxwell's equations to tetrahedral meshes [22, 30]. This approach is accurate on smooth grids, but when the nodal distribution is nonsmooth, the segment connecting two neighbors may not intersect the face of the cell (it is always orthogonal to the plane containing this face) and may in fact intersect this plane outside the face. Several years ago our approach was extended to Voronoi cells [37] for the heat conduction

equation. When we apply our methodology to this mesh it would have the same directions as the methods in [22, 30] for the vector components but the magnetic field would be in a different location. Their magnetic field is defined in the middle of the segment's connecting point to its neighbors but ours is defined in the middle of a cell face. The advantages of our approach are most evident when the methods are applied on extremely rough grids, especially when the properties of the media are discontinuous.

The finite-element method (FEM) (see, for example, [18, 40], and the references therein) have been used extensively to solve Maxwell's equations. From our perspective the main difference between our FDM and FEMs is that in defining our discretizations we have built the discrete analogs of the continuous operators directly into the FDMs so they can be manipulated exactly as the continuous differential operators. Typically, one defines FEMs to discretize the space of solutions. This is in contrast to our FDMs where we directly discretize the differential operators which participate in the formulation of governing equations. The "spirit" of our FDM is close to the original mixed FEM introduced by Raviart and Thomas [31] and Nedelec [27, 1] and the use of vector elements in [18, Chap. 8, pp. 231–280] and the references therein.

3. MAXWELL'S CURL EQUATIONS AND THEIR PROPERTIES

In this paper we consider a nonconducting, free of charge, medium. In this case the governing equations are

$$\frac{\partial \vec{B}}{\partial t} = -\mathbf{curl}\, \vec{E}, \tag{3.1a}$$

$$\frac{\partial \vec{D}}{\partial t} = \mathbf{curl}\, \vec{H}, \tag{3.1b}$$

where $\vec{H}$ is magnetic field intensity, and the dependent equations are

$$\mathbf{div}\, \vec{D} = 0, \tag{3.2a}$$

$$\mathbf{div}\, \vec{B} = 0. \tag{3.2b}$$

If the domain of interest contains more than one media then on the interface between say, medium 1 and medium 2, the tangential component of $\vec{E}$ and the normal component of $\vec{B}$ are continuous;

$$[\vec{n} \times (\vec{E}_1 - \vec{E}_2)] = 0, \qquad (\vec{n}, (\vec{B}_1 - \vec{B}_2)) = 0.$$

If Eq. (3.2b) is initially satisfied then it will hold at later times. This follows if we apply **div** to the left- and right-hand sides of (3.1a) and use the identity $\mathbf{div}\, \mathbf{curl}\, \vec{E} = 0$ to obtain $\partial(\mathbf{div}\, \vec{B})/\partial t = 0$; therefore $\mathbf{div}\, \vec{B} = \text{const} = \mathbf{div}\, \vec{B}|_{t=0} = 0$. Similarly, if (3.2a) is initially satisfied it will hold at later times. This follows from applying **div** to the left- and right-hand sides of (3.1b) and using the identity $\mathbf{div}\, \mathbf{curl}\, \vec{H} = 0$ to obtain $\partial(\mathbf{div}\, \vec{D})\partial t = 0$; therefore $\mathbf{div}\, \vec{D} = \text{const} = \mathbf{div}\, \vec{D}|_{t=0} = 0$.

Therefore, when constructing our FDM we require that the discrete analogs of the identities $\mathbf{div}\, \mathbf{curl}\, \vec{H} = 0$, $\mathbf{div}\, \mathbf{curl}\, \vec{E} = 0$ hold *exactly*, and that discrete analogs of the conditions $\mathbf{div}\, \vec{D} = 0$, $\mathbf{div}\, \vec{B} = 0$ are initially satisfied.

We now consider the law of conservation of electromagnetic energy and analyze the related properties of the differential operators. The energy density of the electromagnetic field is defined as $\frac{1}{2}\{(\vec{E}, \vec{D}) + (\vec{B}, \vec{H})\}$ for a linear and nondispersive medium where ϵ and μ are independent of the field variables and time. The conservation law in electromagnetics (for a nonconducting medium) can be formulated as [32, p. 339]

$$0 = \frac{\partial}{\partial t} \int_V \frac{1}{2}\{(\vec{E}, \vec{D}) + (\vec{B}, \vec{H})\}\, dV + \oint_{\partial V} ([\vec{E} \times \vec{H}], \vec{n})\, dS, \tag{3.3}$$

where $\vec{n}$ is the unit outward normal to the surface ∂V. This equation can be derived by first taking the scalar product of Eq. (3.1b) with $\vec{E}$ and subtracting the resulting equation from the scalar product of Eq. (3.1a) with $\vec{H}$ to obtain

$$(\vec{H}, \mathbf{curl}\, \vec{E}) - (\vec{E}, \mathbf{curl}\, H) = -\left(\vec{H}, \frac{\partial \vec{B}}{\partial t}\right) - \left(\vec{E}, \frac{\partial \vec{D}}{\partial t}\right). \tag{3.4}$$

Then, using the property

$$\frac{\partial}{\partial t}(\vec{E}, \vec{E}) = 2\left(\vec{E}, \frac{\partial \vec{E}}{\partial t}\right) \tag{3.5}$$

and that ϵ and μ are independent of time, we have

$$\left(\vec{E}, \frac{\partial \vec{D}}{\partial t}\right) = \frac{1}{2}\frac{\partial}{\partial t}(\vec{E}, \vec{D}), \qquad \left(\vec{H}, \frac{\partial \vec{B}}{\partial t}\right) = \frac{1}{2}\frac{\partial}{\partial t}(\vec{H}, \vec{B}). \tag{3.6}$$

Next, integrating Eq. (3.4) over the domain V and using (3.6) we obtain

$$\int_V \{(\vec{H}, \mathbf{curl}\, \vec{E}) - (\vec{E}, \mathbf{curl}\, \vec{H})\}\, dV = -\frac{\partial}{\partial t} \int_V \frac{1}{2}\{(\vec{E}, \vec{D}) + (\vec{B}, \vec{H})\}\, dV.$$

The conservation law (3.3) follows from this equation and the identity (1.3) for curls. If the boundary integral in the right-hand side of (1.3) vanishes, then this identity expresses the self-adjointness property of the operator **curl**. Therefore, the discrete analog of this conservation law will hold if the time integration method satisfies a discrete analog of (3.5) and the discrete **curl** satisfies a discrete analog of (1.3).

Because the normal components of $\vec{B}$ and the tangential components of $\vec{E}$ are continuous on discontinuities in the media, we will use them to describe the magnetic flux density and the electric field intensity in the discrete case. Therefore, we solve Maxwell's equations in the form

$$\frac{\partial \vec{B}}{\partial t} = -\mathbf{curl}\, \vec{E}, \tag{3.7a}$$

$$\frac{\partial \vec{E}}{\partial t} = \frac{1}{\epsilon}\, \mathbf{curl}\, \frac{\vec{B}}{\mu}, \tag{3.7b}$$

and impose the divergence-free condition for $\vec{D}$, (3.2a) as

$$\mathbf{div}\, \epsilon \vec{E} = 0. \tag{3.8}$$

In this paper we consider boundary conditions where the tangential component of $\vec{E}$ is given on the boundary,

$$\vec{n} \times \vec{E} = \gamma. \tag{3.9}$$

When $\gamma = 0$, this condition is appropriate for a perfectly conducting surface. The approximation of (3.9) is especially easy for our FDM because we use the tangential components of $\vec{E}$ to describe the electric field. Impedance boundary conditions (see [18, p. 7]) require a combination of the tangential components of $\vec{E}$ and $\vec{H}$ given on the boundary. These boundary conditions can also be treated (see the note at the end of Subsection 5.2).

In this paper we will consider only the "2-D Case," where there are no variations in the electromagnetic fields or geometry in the z direction. That is, all partial derivatives with respect to z are zero, and the domain extends to infinity in the z-direction with no change in the shape or position of its transverse cross section.

In this situation the full set of Maxwell's curl equations can be presented as two groups of equations (see, for example, [42, pp. 54–55]). The first group of equations involves only H_x, H_y, and E_z, and is called the transverse magnetic (TM) mode. The second group of equations involves only E_x, E_y, and H_z, and is called the transverse electric (TE) mode. The TM and TE modes are decoupled and can exist simultaneously with no mutual interaction.

4. SPACES OF DISCRETE FUNCTIONS

4.1. Grid. Consider the logically cuboid grid with hexahedron cells, shown in Fig. 1, where the nodes are enumerated by three indices $(i, j, k) : 1 \le i \le M; 1 \le j \le N; 1 \le k \le O$. Sometimes it is useful to interpret the logically cuboid grid as being formed by intersections of broken lines that approximate the coordinate curves of some underlying curvilinear coordinate system (ξ, η, ζ). The ξ, η, or ζ coordinate corresponds to the grid line where the index i, j, or k is changing, respectively. This interpretation motivates the notation

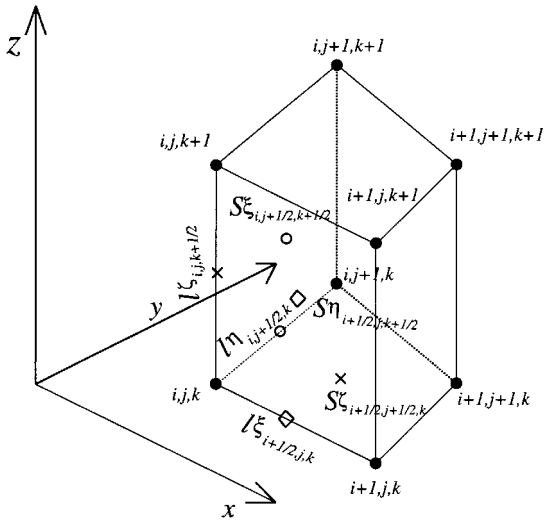

FIG. 1. The elements of the 3-D grid.

we introduce for the areas of faces and lengths of the edges. We denote the length of the edge (i, j, k)—$(i+1, j, k)$ by $l\xi_{i+1/2,j,k}$, the length of the edge (i, j, k)—$(i, j+1, k)$ by $l\eta_{i,j+1/2,k}$, and the length of the edge (i, j, k)—$(i, j, k+1)$ by $l\zeta_{i,j,k+1/2}$. The area of the surface (i, j, k)—$(i, j+1, k)$—$(i, j, k+1)$—$(i, j+1, k+1)$ is denoted by $S\xi_{i,j+1/2,k+1/2}$, the area of surface (i, j, k)—$(i+1, j, k)$—$(i, j, k+1)$—$(i+1, j, k+1)$ is denoted by $S\eta_{i+1/2,j,k+1/2}$, and the area of surface (i, j, k)—$(i+1, j, k)$—$(i+1, j+1, k)$—$(i, j+1, k)$ is denoted by $S\zeta_{i+1/2,j+1/2,k}$. The volume of a 3-D cell is $VC_{i+1/2,j+1/2,k+1/2}$ and the volume relating to the node (see Subsection 4.3 for an explanation why we need one) is denoted by $VN_{i,j,k}$.

4.2. Discrete scalar and vector functions. A discrete scalar function is a function whose domain is the set of multi-indices and range of values is $\mathcal{R}$. For example, if the set of multi-indices is $[(i, j, k)—i = 1, \ldots, M;\ j = 1, \ldots, N;\ k = 1, \ldots, O]$ then the values of the discrete scalar function U are $U_{i,j,k}$. (From here on, we will use the same notation for continuous and discrete functions if it does not lead to ambiguity.) From the formal point of view the discrete scalar function is the vector, whose dimension corresponds to the dimension of a multi-index set. The space of discrete scalar functions consists of all discrete scalar functions with the same domain. The sum of two discrete scalar functions and the multiplication by a scalar are defined in the obvious way: if $W = U + V$ then $W_{i,j,k} = U_{i,j,k} + V_{i,j,k}$, and if $W = \lambda U$ then $W_{i,j,k} = \lambda U_{i,j,k}$. From a formal point of view the space of discrete scalar functions is the usual linear space. We view discrete scalar functions as an approximation to a continuous scalar function where the multi-index corresponds to the particular location on the computational grid. The value of the discrete scalar function is interpreted as an approximate value of a continuous function at this location. For example, we interpret the discrete scalar function with the domain $[(i, j, k) - i = 1, \ldots, M;\ j = 1, \ldots, N; k = 1, \ldots, O]$ as a function whose values are an approximation to the values of a continuous scalar function at the nodes of the computational grid. For this reason we will define the domain of this function as the nodes of the grid, or say that this function is defined at the nodes. We denote this space of discrete scalar functions as HN (here N stands for "node"). In general, we use italics for spaces of scalar functions.

A discrete vector function is the discrete analog of a continuous vector function. It has three components which can be viewed as discrete scalar functions. From a formal point of view, the space of discrete vector functions is the direct sum of linear spaces, that correspond to the discrete scalar functions. For example, we define the discrete vector function $\vec{A} = (AX, AY)^T$; $AX, AY \in HN$. The space of discrete vector functions at the nodes is denoted as $\mathcal{HN}$ (in general, we will use script for spaces of discrete vector functions). Note that formally $\mathcal{HN} = HN \oplus HN$.

We define the space HC (C stands for "cell") as the space where the discrete scalar function U is defined by its values in the cells, $U_{i+1/2,j+1/2,k+1/2}$, and values at the centers of the boundary faces (see [11] for details). We use the cell-centered discretization for scalar functions ϵ and μ that determine the material properties. We define three spaces associated with faces of the cell; the function in the space $HS\xi$ is defined on the ξ faces of the cell; the spaces $HS\eta$ and $HS\zeta$ are defined similarly. There are three spaces associated with the edges of a cell; the function in the space $HL\xi$ is defined on the ξ edges of the cell; the spaces $HL\eta$ and $HL\zeta$ are defined similarly. We consider two different spaces of discrete vector functions. The space $\mathcal{HS} = HS\xi \oplus HS\eta \oplus HS\zeta$ is associated with the discrete representation of a vector function by its orthogonal projections onto the normal

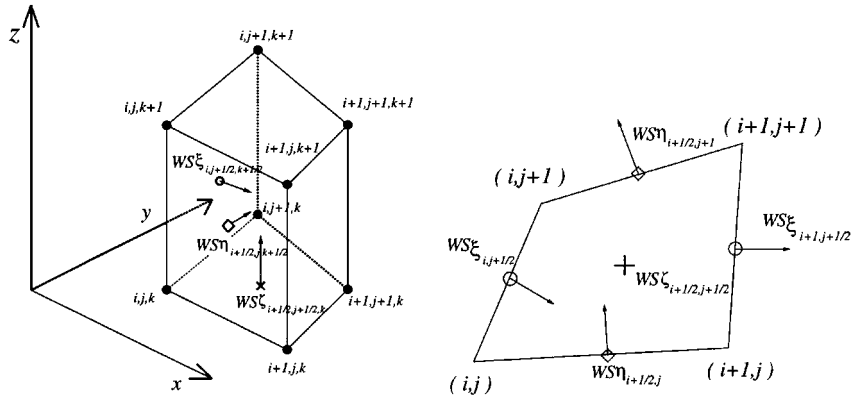

(a) $\mathcal{HS}$ in 3-D (b) $\mathcal{HS}$ in 2-D

FIG. 2. (a) $\mathcal{HS}$ discretization of a vector in three dimensions; (b) The 2-D interpretation of the $\mathcal{HS}$ discretization of a vector results in the face vectors being defined perpendicular to the cell sides and the vertical vectors being defined at cell centers perpendicular to the plane.

of the cell faces (see Fig. 2a). We use this space to describe the discrete magnetic flux $\vec{B}$. The space $\mathcal{HL} = HL\xi \oplus HL\eta \oplus HL\zeta$ is associated with the discrete representation of a vector function by its orthogonal projections onto the direction of the edges (see Fig. 3a). We use this space for the discrete representation of the electric field $\vec{E}$.

In this paper we consider the "2-D" case, where the unknowns depend only on the two spatial coordinates, x and y, even though the vectors may have three components. Formally, 2-D discretizations can be obtained from 3-D discretizations where the ζ-edges are orthogonal to the (x, y) plane and have unit length (see [10], for details). From here on, the discrete values will be independent of the k index and it is dropped from the notation. Also note that for the 2-D case $S\xi_{i,j+1/2} = l\eta_{i,j+1/2}$, $S\eta_{i+1/2,j} = l\xi_{i+1/2,j}$ and $VC_{i+1/2,j+1/2} = S\zeta_{i+1/2,j+1/2}$. The angle between any two adjacent sides of the cell $(i + 1/2,\ j + 1/2)$ that meet at the node $(i',\ j')$ is denoted by $\varphi_{i',j'}^{i+1/2,j+1/2}$.

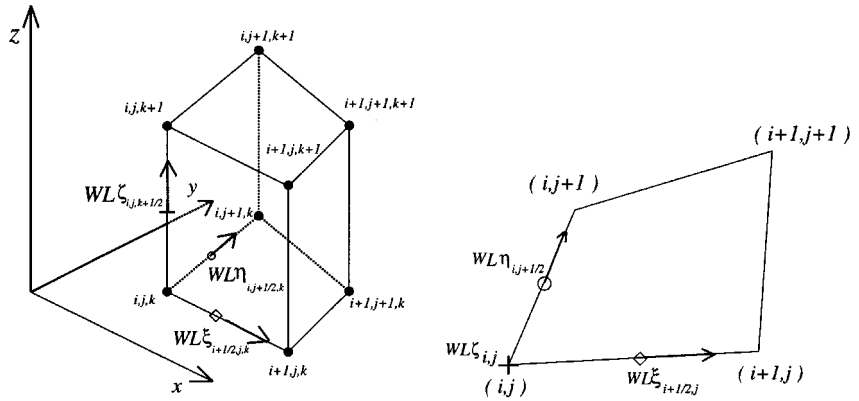

(a) $\mathcal{HL}$ in 3-D (b) $\mathcal{HL}$ in 2-D

FIG. 3. (a) $\mathcal{HL}$ discretization of a vector in three dimensions; (b) 2-D interpretation of the $\mathcal{HL}$ discretization of a vector results in the edge vectors targential to the cell sides and the vertical vectors being defined at cell nodes.

The projection of the 3-D $\mathcal{HS}$ vector discretization space into 2-D results in face vectors perpendicular to the quadrilateral cell sides and cell-centered vertical vectors perpendicular to the 2-D plane (see Fig. 2b). We use the notation

$$BS\xi = \{BS\xi_{(i,j+1/2)} : i = 1, \ldots, M;\ j = 1, \ldots, N-1\},$$
$$BS\eta = \{BS\eta_{(i+1/2,j)} : i = 1, \ldots, M-1;\ j = 1, \ldots, N\},$$
$$BS\zeta = \{BS\zeta_{(i+1/2,j+1/2)} : i = 1, \ldots, M-1;\ j = 1, \ldots, N-1\},$$

and $\vec{B} = (BS\xi, BS\eta, BS\zeta)^T \in \mathcal{HS}$.

The projection of the 3-D $\mathcal{HL}$ vector discretization space into 2-D results in vectors tangential to the quadrilateral cell sides and vertical vectors at the nodes (see Fig. 3b). We use the notation

$$EL\xi = \{EL\xi_{(i+1/2,j)} : i = 1, \ldots, M-1;\ j = 1, \ldots, N\},$$
$$EL\eta = \{EL\eta_{(i,j+1/2)} : i = 1, \ldots, M;\ j = 1, \ldots, N-1\},$$
$$EL\zeta = \{EL\zeta_{(i,j)} : i = 1, \ldots, M;\ j = 1, \ldots, N\},$$

and $\vec{E} = (EL\xi, EL\eta, EL\zeta)^T \in \mathcal{HL}$.

4.3. Discrete inner products. Defining consistent FDMs also requires deriving the appropriate discrete adjoint operators. To define the adjoint operators we must specify the inner products in the spaces of discrete scalar and vector functions. Because the space of discrete scalar functions is the usual linear vector space, we have the usual inner product, $[\cdot, \cdot]$ (which we will call the *formal inner product*), which is just the dot product between vectors in this space. In HC (discrete scalar functions defined in the cell centers), the formal inner product is

$$[U, V]_{HC} \stackrel{\text{def}}{=} \sum_{c \in HC} U_c V_c,$$

where c is multi-index corresponding to cells. From here on, we will use notation $\stackrel{\text{def}}{=}$, when we define a new object. In the space of discrete vector functions $\mathcal{HS} = HS\xi \oplus HS\eta \oplus HS\zeta$, the formal inner product is the sum of the formal inner products of its components

$$[\vec{A}, \vec{B}]_{\mathcal{HS}} \stackrel{\text{def}}{=} \sum_{f\xi \in HS\xi} AS\xi_{f\xi}, BS\xi_{f\xi} + \sum_{f\eta \in HS\eta} AS\eta_{f\eta} BS\eta_{f\eta} + \sum_{f\zeta \in HS\zeta} AS\zeta_{f\zeta} BS\zeta_{f\zeta},$$

where $f\xi$, $f\eta$, and $f\zeta$ are multi-indices for the corresponding families of faces of the cells. Similar definitions hold for the spaces HN and $\mathcal{HL}$.

Because our construction is based on the approximation of the integral identities we introduce additional inner products, $(\cdot, \cdot)$ (which we will call the *natural inner products*), which correspond to the continuous inner products. In the space of discrete scalar functions, HC, the natural inner product corresponding to the continuous inner product $\int_V uv\,dV + \oint_{\partial V} uv\,dS$ is

$$(U, V)_{HC} \stackrel{\text{def}}{=} \sum_{c \in HC} U_c V_c \widetilde{VC}_c,$$

where $\widetilde{VC}_c$ is the volume of the cth cell in the interior of the domain and on the boundary it is equal to the area of boundary face.

We define $\overset{0}{HN}$ to be the subspace of HN where discrete functions are equal to zero on the boundary

$$\overset{0}{HN} \stackrel{\text{def}}{=} \{U \in HN,\, U_{i,j} = 0 \text{ on the boundary}\}$$

(the notation of "zero" above the name of a space indicates the subspace where the functions are equal to zero on the boundary) with natural inner product defined as

$$(U, V)_{\overset{0}{HN}} \stackrel{\text{def}}{=} \sum_{n \in \overset{0}{HN}} U_n V_n V N_n, \tag{4.1}$$

where n is the multi-index corresponding to the nodes and VN_n is the nodal volume.

In the space of vector functions $\mathcal{HS}$, the natural inner product corresponding to the continuous inner product $\int_V (\vec{A}, \vec{B})\, dV$ is

$$(\vec{A}, \vec{B})_{\mathcal{HS}} \stackrel{\text{def}}{=} \sum_{i=1}^{M-1} \sum_{j=1}^{N-1} (\vec{A}, \vec{B})_{(i+1/2,\, j+1/2)}\, VC_{(i+1/2,\, j+1/2)}, \tag{4.2}$$

where $(\vec{A}, \vec{B})$ is the dot product of two vectors. The dot product in the cell is approximated by

$$\begin{aligned}(\vec{A}, \vec{B})_{(i+1/2,\, j+1/2)} = \sum_{k,l=0}^{1} & \frac{V^{(i+1/2,\, j+1/2)}_{(i+k,\, j+l)}}{\sin^2 \varphi^{(i+1/2,\, j+1/2)}_{(i+k,\, j+l)}} \\ & \cdot \Big[AS\xi_{(i+k,\, j+1/2)}\, BS\xi_{(i+k,\, j+1/2)} + AS\eta_{(i+1/2,\, j+l)}\, BS\eta_{(i+1/2,\, j+l)} \\ & + (-1)^{k+l} \big(AS\xi_{(i+k,\, j+1/2)} BS\eta_{(i+1/2,\, j+l)} \\ & + AS\eta_{(i+1/2,\, j+l)} BS\xi_{(i+k,\, j+1/2)} \big) \cos \varphi^{(i+1/2,\, j+1/2)}_{(i+k,\, j+l)} \Big] \\ & + AS\zeta_{i+1/2,\, j+1/2} BS\zeta_{i+1/2,\, j+1/2},\end{aligned} \tag{4.3}$$

where the weights $V^{(i+1/2,\, j+1/2)}_{(i+k,\, j+l)}$ satisfy

$$V^{(i+1/2,\, j+1/2)}_{(i+k,\, j+l)} \geq 0, \qquad \sum_{k,l=0}^{1} V^{(i+1/2,\, j+1/2)}_{(i+k,\, j+l)} = 1. \tag{4.4}$$

In this formula, each index (k, l) corresponds to one of the vertices of the $(i+1/2,\, j+1/2)$ cell, and the notation for the weights is the same as for the angles of a cell. The formula for this dot product is derived in [39, 11].

This dot product is the simplest robust approximation where if a cell angle is close to zero or π (and consequently the coordinate system related to this angle is close to degenerate), then the corresponding weight (and contribution from this vertex) vanishes smoothly when the coordinate system becomes degenerate. Consequently, this dot product can be used for triangular cells that arise as the limit of degenerate quadrilaterals because the unknown component of the vector related to the degenerate vertex does not appear in

either the equation or the dot product. This dot product can also be derived by averaging the dot products corresponding to piece-wise constant vector finite-elements. More accurate approximations for the dot product can be derived using the low-order Raviart–Thomas elements [31, 4] and include terms like $AS\xi_{i,j+1/2}$. $AS\xi_{i+1,j+1/2}$.

The inner product in $\mathcal{HL}$ is similar to the inner product for space $\mathcal{HS}$,

$$(\vec{A}, \vec{B})_{\mathcal{HL}} \stackrel{\text{def}}{=} \sum_{i=1}^{M-1} \sum_{j=1}^{N-1} (\vec{A}, \vec{B})_{(i+1/2,j+1/2)} VC_{(i+1/2,j+1/2)}, \tag{4.5}$$

where $(\vec{A}, \vec{B})_{i+1/2,j+1/2}$ approximates the dot product of two vectors in the cell (see [11]) and looks similar to one for vectors from $\mathcal{HS}$.

The natural and formal inner products satisfy the relationships

$$(U, V)_{HC} = [\mathcal{C}U, V]_{HC} \qquad \text{and} \qquad (\vec{A}, \vec{B})_{\mathcal{HS}} = [S\vec{A}, \vec{B}]_{\mathcal{HS}}, \tag{4.6}$$

where $\mathcal{C} : HC \to HC$ and $\mathcal{S} : \mathcal{HS} \to \mathcal{HS}$ are symmetric positive operators;

$$[\mathcal{C}U, V]_{HC} = [U, \mathcal{C}V]_{HC}, \qquad \text{and} \qquad [\mathcal{C}U, U]_{HC} > 0, \tag{4.7}$$

$$[\mathcal{S}\vec{A}, \vec{B}]_{\mathcal{HS}} = [\vec{A}, \mathcal{S}\vec{B}]_{\mathcal{HS}}, \qquad [\mathcal{S}\vec{A}, \vec{A}]_{\mathcal{HS}} > 0. \tag{4.8}$$

Therefore, the operator $\mathcal{C}$ satisfies the relations

$$(\mathcal{C}U)_c = \widetilde{VC}_c U_c, \qquad c \in HC.$$

The operator $\mathcal{S}$ can be written in block form,

$$\mathcal{S}\vec{A} = \begin{pmatrix} S_{11} & S_{12} & 0 \\ S_{21} & S_{22} & 0 \\ 0 & 0 & S_{33} \end{pmatrix} \begin{pmatrix} AS\xi \\ AS\eta \\ AS\zeta \end{pmatrix} = \begin{pmatrix} S_{11}\, AS\xi + S_{12}\, AS\eta \\ S_{21}\, AS\xi + S_{22}\, AS\eta \\ S_{33}\, AS\zeta \end{pmatrix}. \tag{4.9}$$

By comparing the formal and natural inner products, we can derive the explicit formulas for $\mathcal{S}$ (see [11]). For example, for S_{11} and S_{12} we have

$$(S_{11}\, AS\xi)_{(i,j+1/2)} = \left(\sum_{k=\pm\frac{1}{2}; l=0,1} \frac{V_{(i,j+l)}^{(i+k,j+1/2)}}{\sin^2 \varphi_{(i,j+l)}^{(i+k,j+1/2)}} \right) AS\xi_{(i,j+1/2)}, \tag{4.10}$$

$$\begin{aligned}(S_{12}\, AS\eta)_{(i,j+1/2)} = & \sum_{k=\pm\frac{1}{2}; l=0,1} (-1)^{k+\frac{1}{2}+l} \frac{V_{(i,j+l)}^{(i+k,j+1/2)}}{\sin^2 \varphi_{(i,j+l)}^{(i+k,j+1/2)}} \\ & \times \cos \varphi_{(i,j+l)}^{(i+k,j+1/2)} AS\eta_{(i+k,j+l)}. \end{aligned} \tag{4.11}$$

The operators S_{11}, S_{22}, and S_{33} are diagonal, and the stencils for the operators S_{12} and S_{21} are shown in Fig. 4.

The relationship between the natural and formal inner products in $\overset{0}{HN}$ is

$$(U, V)_{\overset{0}{HN}} = [\mathcal{N}U, V]_{\overset{0}{HN}},$$

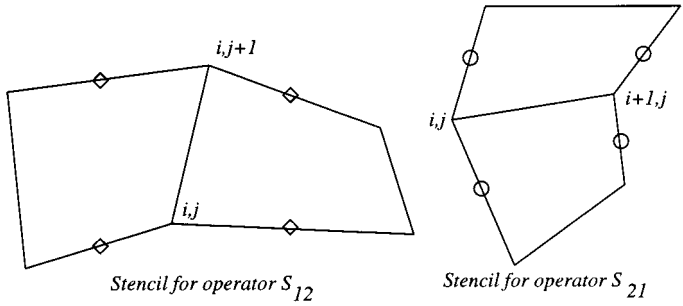

FIG. 4. The stencils of the components S_{12} and S_{21} of the symmetric positive operator S that connects the natural and formal inner products $(\vec{A}, \vec{B})_{\mathcal{HS}} = [\mathcal{S}\vec{A}, \vec{B}]_{\mathcal{HS}}$.

where $\mathcal{N} : HN \to HN$ is a symmetric positive operator in the formal inner product, and

$$(\mathcal{N}U)_n = VN_nU_n, \qquad n \in \overset{0}{HN}$$

The operator $\mathcal{L} : \mathcal{HL} \to \mathcal{HL}$, which connects the formal and natural inner products in $\mathcal{HL}$ (similar to operator $\mathcal{S}$ for space $\mathcal{HS}$), is symmetric and positive and can be written in block form as

$$\mathcal{L}\vec{A} = \begin{pmatrix} L_{11} & L_{12} & 0 \\ L_{21} & L_{22} & 0 \\ 0 & 0 & L_{33} \end{pmatrix} \begin{pmatrix} AL\xi \\ AL\eta \\ AL\zeta \end{pmatrix} = \begin{pmatrix} L_{11}AL\xi + L_{12}AL\eta \\ L_{21}AL\xi + L_{22}AL\eta \\ L_{33}AL\zeta \end{pmatrix}. \tag{4.12}$$

The operators L_{11}, L_{22}, and L_{33} are diagonal, and the stencils for the operators L_{21} and L_{12} are the same as for the operators S_{12} and S_{21} (see Fig. 4). Explicit expressions for these operators are presented in [11].

Natural discrete inner products satisfy the axioms of inner products, that is, they are true inner products and not just approximations of the continuous inner products. Also, discrete spaces are Euclidean spaces.

5. DISCRETE OPERATORS

In this section we consider the discretization of the spatial operators in Maxwell's curl equations, (3.7a), (3.7b), and the divergence-free conditions, (3.2b), and (3.8).

5.1. Discretization of **curl** $\vec{E}$. The discrete analog of **curl** $\vec{E}$ in (3.7a) must act on the discrete electric field, which belongs to $\mathcal{HL}$, where on each edge we have one component of the electric field, which is the orthogonal projection of $\vec{E}$ onto the direction of the edge. For this situation it is natural to use the coordinate invariant definition of the **curl** $\vec{E}$ operator based on Stokes' circulation theorem,

$$(\vec{n}, \mathbf{curl}\, \vec{E}) = \lim_{S \to 0} \frac{\oint_L (\vec{E}, \vec{l})\, dl}{S}. \tag{5.1}$$

Here S is the surface spanning (based on) the closed curve L, $\vec{n}$ is the unit outward normal to S, and $\vec{l}$ is the unit tangential vector to L. In the discrete case the faces of the grid cells will be

the surfaces S in Eq. (5.1) and the "curve" L will be formed by edges of the corresponding face. The range of values of this discrete curl will be the normal components of **curl** $\vec{E}$ given on the faces of the cells (orthogonal projections of **curl** $\vec{E}$ onto the directions of the normals to the cell faces).

Because we are using the normal components of $\vec{B}$ on the cell faces to describe the magnetic flux (space $\mathcal{HS}$), the discrete analogs of both sides of (3.7a) belong to the same discrete space. This construction preserves a discrete analog of Faraday's law of electromagnetic induction locally for each face.

Using the discrete analog of Eq. (5.1), we obtain expressions for components of vector $\vec{R} = (RS\xi, RS\eta, RS\zeta)^T = \mathrm{CURL}\,\vec{E}$, where the discrete natural curl

$$\mathrm{CURL} : \mathcal{HL} \to \mathcal{HS},$$

and

$$RS\xi_{i,j+1/2} = \frac{EL\zeta_{i,j+1} - EL\zeta_{i,j}}{l\eta_{i,j+1/2}}, \qquad RS\eta_{i+1/2,j} = -\frac{EL\zeta_{i+1,j} - EL\zeta_{i,j}}{l\xi_{i+1/2,j}}, \tag{5.2}$$

$$\begin{aligned} RS\zeta_{i+1/2,j+1/2} = {} & \{(EL\eta_{i+1,j+1/2} l\eta_{i+1,j+1/2} - EL\eta_{i,j+1/2} l\eta_{i,j+1/2}) \\ & - \{(EL\xi_{i+1/2,j+1} l\xi_{i+1/2,j+1} - EL\xi_{i+1/2,j} l\xi_{i+1/2,j})\}/S\zeta_{i+1/2,j+1/2} \end{aligned}$$

(see [10] for details).

The expressions for $RS\xi$ and $RS\eta$ contain only the $EL\zeta$ component of $\vec{E}$ and the expression for $RS\zeta$ contains only the $EL\xi$ and $EL\eta$ components. This fact allows us to introduce discrete analogs of the TM and TE modes.

The operator CURL can be presented in (3×3) block form as

$$\mathrm{CURL} = \begin{pmatrix} 0 & 0 & R_{13} \\ 0 & 0 & R_{23} \\ R_{31} & R_{32} & 0 \end{pmatrix}, \tag{5.3}$$

where

$$\begin{aligned} (R_{13}EL\zeta)_{i,j+1/2} &= \frac{EL\zeta_{i,j+1} - EL\zeta_{i,j}}{l\eta_{i,j+1/2}}, \qquad (R_{23}EL\zeta)_{i+1/2,j} = -\frac{EL\zeta_{i+1,j} - EL\zeta_{i,j}}{l\xi_{i+1/2,j}}, \\ (R_{31}EL\xi)_{i+1/2,j+1/2} &= -\frac{EL\xi_{i+1/2,j+1} l\xi_{i+1/2,j+1} - BL\xi_{i+1/2,j} l\xi_{i+1/2,j}}{S\zeta_{i+1/2,j+1/2}}, \\ (R_{32}EL\eta)_{i+1/2,j+1/2} &= \frac{EL\eta_{i+1,j+1/2} l\eta_{i+1,j+1/2} - EL\eta_{i,j+1/2} l\eta_{i,j+1/2}}{S\zeta_{i+1/2,j+1/2}}. \end{aligned} \tag{5.4}$$

This structure of the CURL will be used to derive the discrete adjoint operator $\overline{\mathrm{CURL}}$.

5.2. Discretization of $\frac{1}{\epsilon}$ **curl** $\frac{\vec{B}}{\mu}$. Because of our choice of primary variables, to discretize Eq. (3.7b), we must derive a discrete approximation for the compound operator ${}_{\epsilon}\mathbf{curl}_{\mu} \stackrel{\mathrm{def}}{=} \frac{1}{\epsilon}$ **curl** $\frac{1}{\mu}$. Note that if ϵ and μ are discontinuous and the grid is nonsmooth, then it is not possible to separate them from the **curl** in the discrete approximation.

Because $\vec{E} \in \mathcal{HL}$ and $\vec{B} \in \mathcal{HS}$ the discrete analog of ${}_\epsilon\mathbf{curl}_\mu$ must have $\mathcal{HS}$ as its domain and $\mathcal{HL}$ as its range. To construct the discrete operator with the complimentary domain and range we will use a modification of the identity (1.3) responsible for the conservation of electromagnetic energy. If we consider the identity (1.3) in the subspace of vectors $\vec{A}$ where the surface integral in (1.3) on the right-hand side vanishes and modify it to form the operator ${}_\epsilon\mathbf{curl}_\mu$, we have

$$\int_V \frac{1}{\mu}(\mathbf{curl}\,\vec{E},\vec{B})\,dV = \int_V \epsilon\left(\vec{E},\frac{1}{\epsilon}\,\mathbf{curl}\,\frac{\vec{B}}{\mu}\right)dV. \tag{5.5}$$

That is, ${}_\epsilon\mathbf{curl}_\mu = \mathbf{curl}^*$ in these weighted inner products.

In the discrete case, the modified inner product in $\mathcal{HS}$, $(\cdot,\cdot)^{1/\mu}_{\mathcal{HS}}$, uses the weight $1/\mu$ and the modified inner product in the space $\mathcal{HL}$, $(\cdot,\cdot)^{\epsilon}_{\mathcal{HL}}$, uses the weight ϵ. These modified inner products are defined in [15] when ϵ and μ are general SPD tensors.

The compound discrete adjoint curl, ${}_\epsilon\overline{\mathrm{CURL}}_\mu : \mathcal{HS} \to \mathcal{HL}$ is defined as

$${}_\epsilon\overline{\mathrm{CURL}}_\mu \stackrel{\text{def}}{=} \mathrm{CURL}^* = (\mathcal{L}^\epsilon)^{-1}\cdot \mathrm{CURL}^\dagger \cdot \mathcal{S}^{\frac{1}{\mu}}, \tag{5.6}$$

where $\mathcal{S}^{1/\mu}$ corresponds to the modified inner product in the space $\mathcal{HS}$, and $\mathcal{L}^\epsilon$ corresponds to the modified inner product in the space $\mathcal{HL}$. By definition

$$({}_\epsilon\overline{\mathrm{CURL}}_\mu\,\vec{B},\vec{E})^{\epsilon}_{\mathcal{HL}} = (\mathrm{CURL}\,\vec{E},\vec{B})^{\frac{1}{\mu}}_{\mathcal{HS}}. \tag{5.7}$$

Note that for such definition of ${}_\epsilon\overline{\mathrm{CURL}}_\mu$ both sides of the discrete analog of Eq. (3.7b) are in the same space.

Although CURL is a local operator, the operator ${}_\epsilon\overline{\mathrm{CURL}}_\mu$ is *nonlocal*. We can determine $\vec{\mathrm{C}} = {}_\epsilon\overline{\mathrm{CURL}}_\mu\,\vec{B}$ by solving the system of linear equations

$$\mathcal{L}^\epsilon\vec{\mathrm{C}} = \mathrm{CURL}^\dagger\cdot\mathcal{S}^{\frac{1}{\mu}}\vec{B}, \tag{5.8}$$

with the local operators $\mathcal{L}^\epsilon$ and $\mathrm{CURL}^\dagger\cdot\mathcal{S}^{\frac{1}{\mu}}$.

Using Eq. (5.4) note

$$\mathrm{CURL}^\dagger = \begin{pmatrix} 0 & 0 & R_{31}^\dagger \\ 0 & 0 & R_{32}^\dagger \\ R_{13}^\dagger & R_{23}^\dagger & 0 \end{pmatrix}, \tag{5.9}$$

where

$$\begin{aligned}
\left(R_{31}^\dagger BS\zeta\right)_{i+1/2,j} &= -l\xi_{i+1/2,j}\left(\frac{BS\zeta_{i+1/2,j-1/2}}{S\zeta_{i+1/2,j-1/2}} - \frac{BS\zeta_{i+1/2,j+1/2}}{S\zeta_{i+1/2,j+1/2}}\right)\\
\left(R_{32}^\dagger BS\zeta\right)_{i,j+1/2} &= l\eta_{i,j+1/2}\left(\frac{BS\zeta_{i-1/2,j+1/2}}{S\zeta_{i-1/2,j+1/2}} - \frac{BS\zeta_{i+1/2,j+1/2}}{S\zeta_{i+1/2,j+1/2}}\right),\\
\left(R_{13}^\dagger BS\xi\right)_{i,j} &= \left(\frac{BS\xi_{i,j-1/2}}{l\eta_{i,j-1/2}} - \frac{BS\xi_{i,j+1/2}}{l\eta_{i,j+1/2}}\right),\\
\left(R_{23}^\dagger BS\eta\right)_{i,j} &= -\left(\frac{BS\eta_{i-1/2,j}}{l\xi_{i-1/2,j}} - \frac{BS\eta_{i+1/2,j}}{l\xi_{i+1/2,j}}\right).
\end{aligned}$$

The details of the discretization can be found in [11].

In this paper we consider problems where the tangential components of $\vec{E}$ are given on the boundary. There are other types of boundary conditions, such as impedance boundary conditions, where the tangential components $[\vec{H} \times \vec{n}]$ must be approximated on the boundary. For this case the boundary integral in the identity (1.3) does not vanish. The operator **curl** $\vec{E}$ is adjoint to the extended curl operator which is **curl** $\vec{H}$ in the interior and is the tangential component of $\vec{H}$ on the boundary. For these types of boundary conditions we must also introduce an inner product in the space $\mathcal{HL}$ which includes the boundary integral (see [13]).

5.3. *Discretization of* **div** $\vec{B}$. To discretize **div** $\vec{B}$ in the divergence-free condition (3.2b) we use the coordinate invariant definition of the **div** operator based on Gauss' divergence theorem,

$$\mathbf{div}\,\vec{B} = \lim_{V \to 0} \frac{\oint_{\partial V} (\vec{B}, \vec{n})\, dS}{V}, \tag{5.10}$$

where $\vec{n}$ is the unit outward normal to the boundary ∂V. In the discrete case, V is the volume of the grid cell and ∂V is the set of faces of the cell.

The natural domain for the discrete operator is the space $\mathcal{HS}$ and the natural range is HC,

$$\mathrm{DIV} : \mathcal{HS} \to HC, \tag{5.11}$$

$$\begin{aligned}(\mathrm{DIV}\,\vec{B})_{(i+1/2,\,j+1/2)} &= \frac{1}{VC_{(i+1/2,\,j+1/2)}} \Big\{ \big(BS\xi_{(i+1,\,j+1/2)} S\xi_{(i+1,\,j+1/2)} - BS\xi_{(i,\,j+1/2)} S\xi_{(i,\,j+1/2)} \big) \\ &\quad + \big(BS\eta_{(i+1/2,\,j+1)} S\eta_{(i+1/2,\,j+1)} - BS\eta_{(i+1/2,\,j)} S\eta_{(i+1/2,\,j)} \big) \Big\}. \end{aligned} \tag{5.12}$$

The details can be found in [10], where it is also shown that DIV CURL $\vec{E} \equiv 0$. Therefore, the discrete analog of the divergence-free condition (3.2b) will hold in grid cells.

5.4. *Discretization of* **div** $\epsilon\vec{E}$. Because $\vec{E} \in \mathcal{HL}$, we construct the compound discrete operator $\overline{\mathrm{DIV}}^{\epsilon} : \mathcal{HL} \to HN$ to discretize divergence-free condition (3.8). To define $\overline{\mathrm{DIV}}^{\epsilon}$ we consider the identity (1.4) in the subspace of scalar functions, $\overset{0}{H}$, where $u(x, y) = 0$, $(x, y) \in \partial V$, where the boundary term is zero, and modify the resulting identity by changing $\vec{W}$ to $\epsilon\vec{W}$:

$$\int_V \epsilon(\vec{W}, \mathbf{grad}\, u)\, dV = -\int_V u\, \mathbf{div}^{\epsilon}\, \vec{W}\, dV. \tag{5.13}$$

That is, the operator $\mathbf{div}^{\epsilon}$ is the negative adjoint to **grad** in the inner products

$$(u, v)_{\overset{0}{H}} = \int_V uv\, dV, \qquad \text{and} \qquad (\vec{A}, \vec{C})^{\epsilon}_{\mathcal{H}} \overset{\text{def}}{=} \int_V \epsilon(\vec{A}, \vec{C})\, dV. \tag{5.14}$$

We also will construct a discrete analog of the compound operator $\mathbf{div}^{\epsilon}$ as the negative adjoint to the discrete **grad**. Because the domain of the discrete $\mathbf{div}^{\epsilon}$ is $\mathcal{HL}$, the range of the discrete **grad** also must be $\mathcal{HL}$.

This discrete **grad** is derived using the identity where for any direction l given by the unit vector $\vec{l}$, the directional derivative can be defined as

$$\frac{\partial u}{\partial l} = (\mathbf{grad}\, u, \vec{l}), \tag{5.15}$$

which is the orthogonal projection of **grad** u onto direction given by $\vec{l}$.

In the discrete case for a function $U \in HN$, this relationship leads to the coordinate invariant definition of the natural discrete gradient operator:

$$\mathrm{GRAD}: HN \to \mathcal{HL}. \tag{5.16}$$

The vector $\vec{G} = \mathrm{GRAD}\, U$ is defined as

$$GL\xi_{i+1/2,j} = \frac{U_{i+1,j} - U_{i,j}}{l\xi_{i+1/2,j}}, \qquad GL\eta_{i,j+1/2} = \frac{U_{i,j+1} - U_{i,j}}{l\eta_{i,j+1/2}}, \qquad GL\zeta_{i,j} = 0. \tag{5.17}$$

The operator $\overline{\mathrm{DIV}}^{\epsilon}: \mathcal{HL} \to HN$ is defined as

$$\overline{\mathrm{DIV}}^{\epsilon} \stackrel{\mathrm{def}}{=} -\mathrm{GRAD}^{*} = -\mathcal{N}^{-1} \cdot \mathrm{GRAD}^{\dagger} \cdot \mathcal{L}^{\epsilon}, \tag{5.18}$$

where $\mathcal{N}^{-1}$, $\mathrm{GRAD}^{\dagger}$, and L^{ϵ} are local operators (see [11] for details). The stencil for $\overline{\mathrm{DIV}}^{\epsilon}$ is shown in Fig. 5.

To verify that Gauss' law holds in the discrete case, we confirm that $\overline{\mathrm{DIV}}^{\epsilon} \cdot_{\epsilon} \overline{\mathrm{CURL}}_{\mu} = 0$ by noting

$$\begin{aligned} \overline{\mathrm{DIV}}^{\epsilon} \cdot_{\epsilon} \overline{\mathrm{CURL}}_{\mu} &= -N^{-1} \cdot \mathrm{GRAD}^{\dagger} \cdot \mathcal{L}^{\epsilon} \cdot (\mathcal{L}^{\epsilon})^{-1} \cdot \mathrm{CURL}^{\dagger} \cdot \mathcal{S}^{\frac{1}{\mu}} \\ &= -N^{-1} \cdot \mathrm{GRAD}^{\dagger} \cdot \mathrm{CURL}^{\dagger} \cdot \mathcal{S}^{\frac{1}{\mu}}, \end{aligned}$$

and $\mathrm{GRAD}^{\dagger} \cdot \mathrm{CURL}^{\dagger} \equiv 0$ (see [11]).

Because the range of values of $\overline{\mathrm{DIV}}^{\epsilon}$ is HN, the discrete analog of the divergence-free condition (3.8) holds at the nodes.

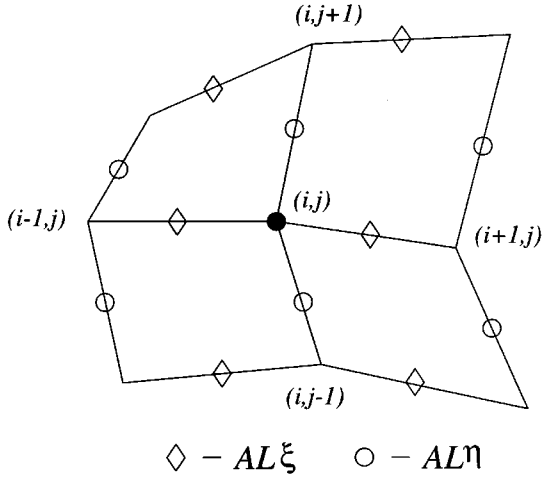

FIG. 5. Stencil for the operator $\overline{\mathrm{DIV}}^{\epsilon} = -\mathrm{GRAD}^{*}: \mathcal{HL} \to \overset{0}{HN}$.

6. FINITE-DIFFERENCE METHOD

6.1. Maxwell's curl equations. We first consider the discrete space-continuous time equations

$$\frac{\partial \vec{B}}{\partial t} = -\mathrm{CURL}\,\vec{E}, \tag{6.1a}$$

$$\frac{\partial \vec{E}}{\partial t} = {}_{\epsilon}\overline{\mathrm{CURL}}_{\mu}\,\vec{B}, \tag{6.1b}$$

where the discrete operators CURL and ${}_{\epsilon}\overline{\mathrm{CURL}}_{\mu}$ are defined in Subsections 5.1 and 5.2, respectively.

To analyze the law of conservation of electromagnetic energy for Eqs. (6.1a), (6.1b), note that the electric and magnetic part of the energy can be expressed in terms of our primary variables $\vec{E}$ and $\vec{B}$ as

$$\int_V (\vec{D}, \vec{E})\,dV = \int_V \epsilon(\vec{E}, \vec{E})\,dV, \qquad \int_V (\vec{B}, \vec{H})\,dV = \int_V \frac{1}{\mu}(\vec{B}, \vec{B})\,dV.$$

The discrete analog of the electromagnetic energy is

$$\mathcal{E}^h_{EH} = \frac{1}{2}\big[(\vec{E}, \vec{E})^{\epsilon}_{\mathcal{HL}} + (\vec{B}, \vec{B})^{\frac{1}{\mu}}_{\mathcal{HL}}\big]. \tag{6.2}$$

Taking the inner product $(\cdot,\cdot)^{1/\mu}_{\mathcal{HS}}$ of $\vec{B}$ with both sides of (6.1a) and similarly for (6.1b) we obtain

$$\left(\frac{\partial \vec{B}}{\partial t}, \vec{B}\right)^{\frac{1}{\mu}}_{\mathcal{HS}} = -(\mathrm{CURL}\,\vec{E}, \vec{B})^{\frac{1}{\mu}}_{\mathcal{HS}}, \qquad \left(\frac{\partial \vec{E}}{\partial t}, \vec{E}\right)^{\epsilon}_{\mathcal{HL}} = ({}_{\epsilon}\overline{\mathrm{CURL}}_{\mu}\,\vec{B}, \vec{E})^{\epsilon}_{\mathcal{HL}}.$$

By adding these two equations,

$$\frac{\partial \mathcal{E}^h_{EH}}{\partial t} = -(\mathrm{CURL}\,\vec{E}, \vec{B})^{\frac{1}{\mu}}_{\mathcal{HS}} + ({}_{\epsilon}\overline{\mathrm{CURL}}_{\mu}\,\vec{B}, \vec{E})^{\epsilon}_{\mathcal{HL}}, \tag{6.3}$$

and using (5.7), we note that the right side of this equation is zero. This corresponds to the preservation of energy when the tangential component of $\vec{E}$ is zero on the boundary. For the general case, in correspondence with (1.3), the right side of the equation will be equal to a discrete approximation of corresponding the boundary integral. Thus the conservation of electromagnetic energy for the discrete model is the result of the consistent and compatible construction of the discrete curl operators.

The time discretization method

$$\frac{\vec{B}^{n+1} - \vec{B}^n}{\Delta t} = -\mathrm{CURL}\,\vec{E}^{\alpha_1}, \tag{6.4a}$$

$$\frac{\vec{E}^{n+1} - \vec{E}^n}{\Delta t} = {}_{\epsilon}\overline{\mathrm{CURL}}_{\mu}\,\vec{B}^{\alpha_2}, \tag{6.4b}$$

where $\vec{E}^{\alpha_1} = \alpha_1\vec{E}^{n+1} + (1-\alpha_1)\vec{E}^n$ and $\vec{B}^{\alpha_2} = \alpha_2\vec{B}^{n+1} + (1-\alpha_2)\vec{B}^n$, and $t_n = \Delta t n$, includes both explicit and implicit methods.

Traditionally, because system (1.1) is hyperbolic, either the stable explicit method ($\alpha_1 = 0$ or $\alpha_2 = 0$) or the explicit leapfrog method [20, 23] is used. For some problems, especially those with strongly discontinuous coefficients, it is important to preserve energy. The only scheme of form (6.4a), (6.4b) which preserves energy is the second order implicit midpoint method ($\alpha_1 = \alpha_2 = 0.5$). Also, there are situations when the increased stability of an implicit method is necessary to avoid taking extremely small time steps. This situation occurs when computing the motion of fully electromagnetic particles in the implosion of a laser fusion capsule [1].

To prove that the midpoint method is conservative take the inner product of Eq. (6.4a) with $\vec{B}^{0.5}$ and the second equation with $\vec{E}^{0.5}$. We obtain

$$\frac{\left(\mathcal{E}_{EH}^h\right)^{n+1} - \left(\mathcal{E}_{EH}^h\right)^n}{\Delta t} = -(\mathrm{CURL}\,\vec{E}^{0.5}, \vec{B}^{0.5})_{\mathcal{HS}}^{\frac{1}{\mu}} + \left({}_{\epsilon}\overline{\mathrm{CURL}}_{\mu}\vec{B}^{0.5}, \vec{E}^{0.5}\right)_{\mathcal{HL}}^{\epsilon}. \quad (6.5)$$

By construction, the right-hand side of this equation reduces to a discrete analog of a boundary integral and guarantees the method is conservative. There is an $O(\Delta t)$ conservation error for any other choice of α's.

The discrete form of the "divergence-free" conditions (3.8), (3.2b) is

$$\overline{\mathrm{DIV}}^{\epsilon}\vec{E}^n = 0, \quad (6.6a)$$

$$\mathrm{DIV}\,\vec{B}^n = 0, \quad (6.6b)$$

where $\overline{\mathrm{DIV}}^{\epsilon}$ and DIV are defined by Eqs. (5.18) and (5.12), respectively.

To prove that if (6.6a), (6.6b) are satisfied initially, then they will be satisfied at later times, we first apply DIV to both sides of Eq. (6.4a),

$$\frac{\mathrm{DIV}\,\vec{B}^{n+1} - \mathrm{DIV}\,\vec{B}^n}{\Delta t} = -\mathrm{DIV}\,\mathrm{CURL}\,\vec{E}^{\alpha_1} = 0. \quad (6.7)$$

Therefore

$$\mathrm{DIV}\,\vec{B}^{n+1} = \mathrm{DIV}\,\vec{B}^0 = 0. \quad (6.8)$$

Similarly applying $\overline{\mathrm{DIV}}^{\epsilon}$ to (6.4b) and using $\overline{\mathrm{DIV}}^{\epsilon}\,{}_{\epsilon}\overline{\mathrm{CURL}}_{\mu} \equiv 0$,

$$\overline{\mathrm{DIV}}^{\epsilon}\vec{E}^{n+1} = \overline{\mathrm{DIV}}^{\epsilon}\vec{E}^0 = 0. \quad (6.9)$$

Therefore, if the discrete divergence-free conditions are satisfied initially they will hold for later times.

Let us now consider TM and TE modes of our discrete equations (6.4a), (6.4b). The TM-mode equations for the $BS\xi$, $BS\eta$ components of the magnetic flux and the $EL\zeta$ component of the electric field are

$$\frac{BS\xi^{n+1} - BS\xi^n}{\Delta t} = -R_{13}EL\zeta^{\alpha_1}, \qquad \frac{BS\eta^{n+1} - BS\eta^n}{\Delta t} = -R_{23}EL\zeta^{\alpha_1},$$

$$L_{33}^{\epsilon}\frac{EL\zeta^{n+1} - EL\zeta^n}{\Delta t} = \left(R\dagger_{13}\cdot S_{11}^{\frac{1}{\mu}} + R_{23}^{\dagger}\cdot S_{21}^{\frac{1}{\mu}}\right)BS\xi^{\alpha_2} + \left(R\dagger_{13}\cdot S_{12}^{\frac{1}{\mu}} + R_{23}^{\dagger}\cdot S_{22}^{\frac{1}{\mu}}\right)BS\eta^{\alpha_2}.$$

The TE-mode equations for the $BS\zeta$ component of the magnetic flux and the $EL\xi$, $EL\eta$ components of the electric field are

$$\frac{BS\zeta^{n+1} - BS\zeta^n}{\Delta t} = -\big(R_{31}\, EL\xi^{\alpha_1} + R_{32} EL\eta^{\alpha_1}\big),$$
$$L^{\epsilon}_{11}\frac{EL\xi^{n+1} - EL\xi^n}{\Delta t} + L^{\epsilon}_{12}\frac{EL\eta^{n+1} - EL\eta^n}{\Delta t} = R^{\dagger}_{31} S^{\frac{1}{\mu}}_{33} BS\zeta^{\alpha_2},$$
$$L^{\epsilon}_{21}\frac{EL\xi^{n+1} - EL\xi^n}{\Delta t} + L^{\epsilon}_{22}\frac{EL\eta^{n+1} - EL\eta^n}{\Delta t} = R^{\dagger}_{32} S^{\frac{1}{\mu}}_{33} BS\zeta^{\alpha_2}.$$

7. SOLUTION PROCEDURE

When $\alpha_1, \alpha_2 \neq 0$ then the integration method is implicit and on every time step we must solve the system of linear equations (6.4a), (6.4b). This system can be written as

$$\vec{B}^{n+1} = -\Delta t \alpha_1 \,\mathrm{CURL}\, \vec{E}^{n+1} + \vec{F}_B(\vec{B}^n, \vec{E}^n), \tag{7.1}$$
$$\mathcal{L}^{\epsilon} \vec{E}^{n+1} = \Delta t \alpha_2 \,\mathrm{CURL}^{\dagger} \cdot \mathcal{S}^{\frac{1}{\mu}} \vec{B}^{n+1} + \vec{F}_E(\vec{B}^n, \vec{E}^n), \tag{7.2}$$

where

$$\vec{F}_B(\vec{B}^n, \vec{E}^n) = \vec{B}^n - \Delta t(1-\alpha_1)\,\mathrm{CURL}\, \vec{E}^n, \tag{7.3}$$
$$\vec{F}_E(\vec{B}^n, \vec{E}^n) = \mathcal{L}^{\epsilon} \vec{E}^n + \Delta t(1-\alpha_2)\,\mathrm{CURL}^{\dagger} \cdot \mathcal{S}^{\frac{1}{\mu}} \vec{B}^n, \tag{7.4}$$

are known. We can easily eliminate $\vec{B}^{n+1}$ and obtain a single second-order equation for $\vec{E}^{n+1}$,

$$\mathcal{A}\vec{E}^{n+1} \stackrel{\mathrm{def}}{=} \big(\mathcal{L}^{\epsilon} + (\Delta t)^2 \alpha_1 \alpha_2 \,\mathrm{CURL}^{\dagger} \cdot \mathcal{S}^{\frac{1}{\mu}} \cdot \mathrm{CURL}\big)\vec{E}^{n+1} = \vec{F}(\vec{B}^n, \vec{E}^n), \tag{7.5}$$

where

$$\vec{F}(\vec{B}^n, \vec{E}^n) = \vec{F}_E(\vec{B}^n, \vec{E}^n) + \Delta t \alpha_2 \,\mathrm{CURL}^{\dagger} \cdot \mathcal{S}^{\frac{1}{\mu}} \vec{F}_B(\vec{B}^n, \vec{E}^n) \tag{7.6}$$

is known. The operator $\mathcal{A}$ defined by (7.5) is SPD, which follows from its structure and properties of operators $\mathcal{L}^{\epsilon}$ and $\mathcal{S}^{\frac{1}{\mu}}$.

Equation (7.5) contains both the TM and TE modes. The TM equation is a "scalar" equation for $EL\zeta$ and can be solved effectively by any preconditioned iterative method which takes advantage of SPD property. The TE equation is a block, (2×2) SPD system for $EL\xi$ and $EL\eta$ with a structure very close to the system arising for the heat flux in the heat conduction equation solved in [39, 15, 26], and one can use the iterative methods described in these papers to solve this system.

Once (7.5) has been solved, $\vec{B}^{n+1}$ is explicitly defined by (7.1). This solution procedure guarantees that the discrete analog of Faraday's law is satisfied exactly, independent of how accurate (7.5) is solved (see [36] for a general discussion on violation of conservation properties when solving difference equations by iterative methods).

8. NUMERICAL EXAMPLES

In this section, we demonstrate the effectiveness of our approach for solving Maxwell's curl equations for the TE mode.

We integrate Maxwell's curl equations with conservative mid-point method ($\alpha_1 = \alpha_2 = 0.5$) and a time step sufficiently small so the time errors are much smaller than the spatial discretization errors. All the parameters in this subsection are given in MKS units and the free space constants are $\epsilon_0 = 8.85 \times 10^{-12}$ and $\mu_0 = 1.2566 \times 10^{-6}$.

8.1. Reflection and refraction at the boundary of two nonconducting media: Normal incidence. The reflection and refraction of the pulse at the boundary of two nonconducting media [32, pp. 382–385] are the one-dimensional problem when the incident pulse is normal to the interface. We solve this problem in a 2-D rectangular domain $[-1, 1] \times [0, 1]$, where interface between two media coincides with the y axis. The permittivities in the "left" and "right" media are $\epsilon_1 = k_1\epsilon_0$, $\epsilon_2 = k_2\epsilon_0$, and $\mu = \mu_0$ for both media. The indices of refraction are $n_1 = \sqrt{k_1}$, $n_2 = \sqrt{k_2}$. In our calculations we took $k_1 = 1$ and $k_2 = 2$.

The incident wave is

$$E_y^{inc}(x, t) = A_E^{inc} g((t - \sqrt{\mu_0\epsilon_1}(x + 1)) * 10^9), \tag{8.1a}$$

$$H_z^{inc}(x, t) = A_H^{inc} g((t - \sqrt{\mu_0\epsilon_1}(x + 1)) * 10^9), \tag{8.1b}$$

where g is the pulse function

$$g(s) = \begin{cases} 1 - \cos(2\pi s), & 0 \le s \le 1 \\ 0, & \text{elsewhere} \end{cases}, \tag{8.2}$$

and the amplitudes are

$$A_E^{inc} = 0.5\sqrt{\frac{\mu_0}{\epsilon_1}}, \qquad A_H^{inc} = A_E^{inc} n_1 \sqrt{\frac{\epsilon_0}{\mu_0}}. \tag{8.3}$$

This wave is generated by imposing boundary conditions for E_y at $x = -1$

$$E_y|_{x=-1} = A_E^{inc} g(t * 10^9). \tag{8.4}$$

The incident wave reaches the boundary between the two materials at time $t^* = \sqrt{\mu_0\epsilon_1} = 3.3348 * 10^{-9}$.

Until the transmitted or reflected waves reach the computational boundaries the exact solution [32, pp. 382–385] for the "left" media, $-1 \le x \le 0$, is the sum of incident wave and reflected wave and for "right" media, $0 \le x \le 1$, is the transmitted wave.

The exact and 1-D approximate solutions ($M = 129$), which play the reference role for 2-D computations, for the characteristic time moments are presented in Fig. 6. The numerical method accurately approximates the pulse traveling in a homogeneous media [$t = 2 \times 10^{-9}$, (a)], during the interaction with the discontinuity [$t = 4 \times 10^{-9}$, (b)] and the shape and velocity of the transmitted and reflected waves [$t = 6 \times 10^{-9}$, (c)].

In two dimensions, because this example is posed for the TE mode, the magnetic field has just one component H_z which is measured in the center of the 2-D cell. Because μ is also given in the center of the cell, we can easily extract H_z from $B_z = \mu H_z$, which is our primary variable in the numerical method. Note that $\vec{E} \equiv 0$ at $t = 0$ and therefore the divergence-free condition for $\vec{D}$ is satisfied.

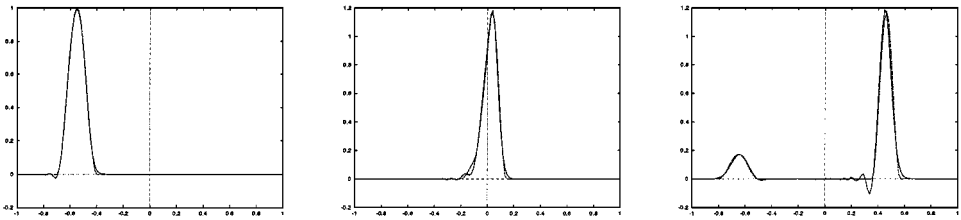

FIG. 6. Exact and 1-D approximate solutions for the H_z component of magnetic field ($M = 129$) at (a) $t = 2 \times 10^{-9}$, (b) $t = 4 \times 10^{-9}$, and (c) $t = 6 = 10^{-9}$.

We solved this problem on both smooth and random grids, Fig. 7. The smooth grid is obtained by the mapping of a uniform (ξ, η) grid in $[-1, 1] \times [0, 1]$ into the same computational space $x(\xi, \eta)$, $y(\xi, \eta)$ by

$$x(\xi, \eta) = \xi + 0.1 \sin(2\pi\xi) \sin(2\pi\eta), \qquad y(\xi, \eta) = \eta + 0.1 \sin(2\pi\xi) \sin(2\pi\eta).$$

The nonsmooth grid (random grid) is obtained by moving nodes in a uniform square grid in random directions and with a random amplitude equal to 20% of initial grid size.

To measure the accuracy of the 2-D calculations, we compare the values of H_z as a function of time for the 1-D and 2-D calculations at a fixed position. In 1-D we plot the solution at the cell center closest to $x = 0.1$. In 2-D we plot the solution at the cell center closest to (0.1, 0). These values plotted in Fig. 8 demonstrate that behavior of 1-D and 2-D solutions is close. In Fig. 9 the straight contour lines illustrate how well the 2-D approximate solution for H_z preserves the one-dimensional shape on the nonuniform smooth grid.

We also calculated the convergence rate in the discrete max and L_2 norms on a sequence of refined grids. The error for $H_z = HS\zeta$ is defined as

$$\mathbf{\Psi}^H_{i+1/2,\,j+1/2} = HS\zeta_{i+1/2,\,j+1/2} - HS\zeta^{exact}\left(x^c_{i+1/2,\,j+1/2}, y^c_{i+1/2,\,j+1/2}\right), \qquad (8.5)$$

where $(x^c_{i,j}, y^c_{i,j})$ is the geometrical center of the $(i + 1/2,\ j + 1/2)$ cell. The norms of $\mathbf{\Psi}_H$ are defined as

$$\|\mathbf{\Psi}^H\|_{\max} = \max_{i,j} |\mathbf{\Psi}^H_{i,j}|, \qquad \|\mathbf{\Psi}^H\|_{L_2} = \sqrt{(\mathbf{\Psi}^H, \mathbf{\Psi}^H)_{HC}}.$$

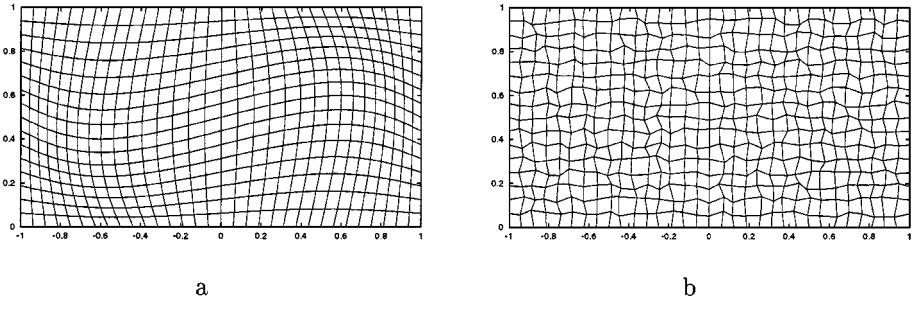

FIG. 7. Computational grids (33×17); (a) smooth grid, (b) random grid.

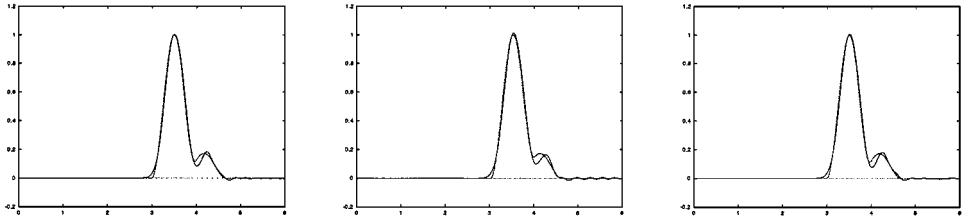

FIG. 8. Component H_z as a function of time; approximate solution, — solid line; (a) 1-D case, $M = 129$, (b) 2-D case, smoth grid, $M = 129$, $N = 65$; (c) 2-D case, random grid, $M = 129$, $N = 65$.

For $\vec{E} = (EL\xi, EL\eta)$ the errors are defined as

$$\mathbf{\Psi}^{EL\xi}_{i+1/2,j} = EL\xi_{i+1/2,j} - EL\xi^{exact}\big(x^{\xi}_{i+1/2,j}, y^{\xi}_{i+1/2,j}\big), \tag{8.6a}$$

$$\mathbf{\Psi}^{EL\eta}_{i,j+1/2} = EL\xi_{i,j+1/2} - EL\eta^{exact}\big(x^{\eta}_{i,j+1/2}, y^{\eta}_{i,j+1/2}\big), \tag{8.6b}$$

where $EL\xi^{exact}$ and $EL\eta^{exact}$ are projections of the exact solution to the edges and $(x^{\xi}_{i+1/2,j}, y^{\xi}_{i+1/2,j})$ and $(x^{\eta}_{i,j+1/2}, y^{\eta}_{i,j+1/2})$ are the coordinates of the mid-points of the edges. The norms for $\vec{\mathbf{\Psi}}^E = (\mathbf{\Psi}^{EL\xi}, \vec{\mathbf{\Psi}}^{EL\eta})$ are defined as

$$\|\vec{\mathbf{\Psi}}^E\|_{\max} = \max_{i,j}\big[\max\big(\big|\mathbf{\Psi}^{EL\xi}_{i+1/2,j}\big|, \big|\mathbf{\Psi}^{EL\eta}_{i,j+1/2}\big|\big)\big], \qquad \|\vec{\mathbf{\Psi}}^E\|_{L_2} = \sqrt{\vec{\mathbf{\Psi}}^E, \vec{\mathbf{\Psi}}^E)_{\mathcal{HL}}}.$$

The errors at $t = 4 \times 10^{-9}$ in Table I show that the L_2 and max norm convergence rates for both smooth and random grids are between first and second order. Our convergence analysis for the 1-D case (not presented here) is in close agreement with these 2-D results.

These results verify the effectiveness of the method for problems with discontinuous coefficients on nonsmooth, nonorthogonal grids.

8.2. Scattering of a plane wave on perfect conductor. Our next example is an infinite domain problem modeling the scattering of a plane wave on a perfect conductor [20, 23].

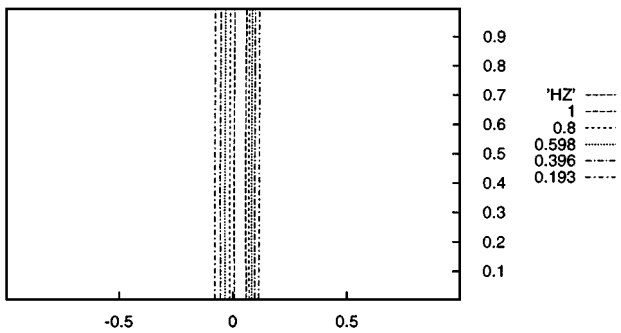

FIG. 9. Isolines of H_z at $t = 4 \times 10^{-9}$, for smooth grid, $M = 129$, $N = 65$.

TABLE I
The Errors for Wave Reflection and Refraction at the Boundary of Two Nonconducting Media at $t = 4 \times 10^{-9}$

M/N	Norm	Smooth $\vec{H}$	Grid $\vec{E}$	Nonsmooth $\vec{H}$	Grid $\vec{E}$
33/17	L_2	0.209	8.09E-2	0.199	8.26E-2
	max	0.532	0.230	0.484	0.219
65/33	L_2	9.13E-2	3.23E-2	9.19E-2	3.21E-2
	max	0.307	0.110	0.250	0.105
129/65	L_2	3.01E-2	8.57E-3	2.91E-2	8.42E-3
	max	0.120	3.30E-2	0.106	3.38E-2
Conv. rate	L_2	1.60	1.91	1.65	1.93
	max	1.35	1.73	1.23	1.63

Note. For each grid size in the top sub-row we present the L_2 error, and in the bottom sub-row we present the max error. In the very bottom we present the estimation for convergence rate for both norms.

We consider a plane wave

$$\vec{E}(x,t) = \begin{pmatrix} 0 \\ \sqrt{\mu_0/\epsilon_0}\, g((t-(x+0.1)\sqrt{\epsilon_0\mu_0})10^9) \end{pmatrix} \tag{8.7a}$$

$$H_z(x,t) = g((t-(x+0.1)\sqrt{\epsilon_0\mu_0})10^9) \tag{8.7b}$$

incident to a perfectly conducting circular cylinder of radius 0.1 m centered at the origin. Our media is "free space" with $\epsilon = \epsilon_0$ and $\mu = \mu_0$. Here the impulse $g(s)$ has the form

$$g(s) = \begin{cases} [\exp(-10(s-1)^2) - \exp(-10)]/[1-\exp(-10)], & 0 \le s \le 2 \\ 0 & \text{otherwise.} \end{cases}$$

The numerical domain is an annulus with inner radius 0.1 m and outer radius 1.1 m. Because the problem is symmetric about the x-axis, we solve the problem in the half domain $\Omega = \{(x,y) \in (0.1 < \sqrt{x^2+y^2} < 1.1) \times (y > 0)\}$. We define the tangential component of $\vec{E}$ to be zero on all boundaries except the surface of the inner cylinder, where we define the tangential component of $\vec{E}$ to equal the tangential component of the incident wave (see [20] for details). That is, we solve for the scattered (i.e., total minus incident) field. These boundary conditions are valid until $t = 4$ ns, when the boundary condition on the outer cylinder starts to generate spurious reflections. The initial conditions correspond to the time when the incident wave (traveling from left to right) just arrives at the inner cylinder. Therefore, initially there are no scattered waves and the electric and magnetic fields are zero, and therefore the divergence-free condition for $\vec{D}$ is satisfied.

The problem is solved on the uniform polar grid (see Fig. 10) with 31 nodes in r and 16 nodes in θ. In Fig. 11 the magnetic field is plotted as a function of time at the two observation points indicated in Fig. 10. The results are almost identical with results in [23, Fig. 7]. Similar to [23] we observe second order convergence in the spatial error.

In Fig. 12, we show the electric vector field at $t = 4$ ns for $M = 40$, $N = 64$. The numerical solution is free of spurious solutions and the divergence-free condition for $\vec{D}$ is satisfied exactly at the internal nodes.

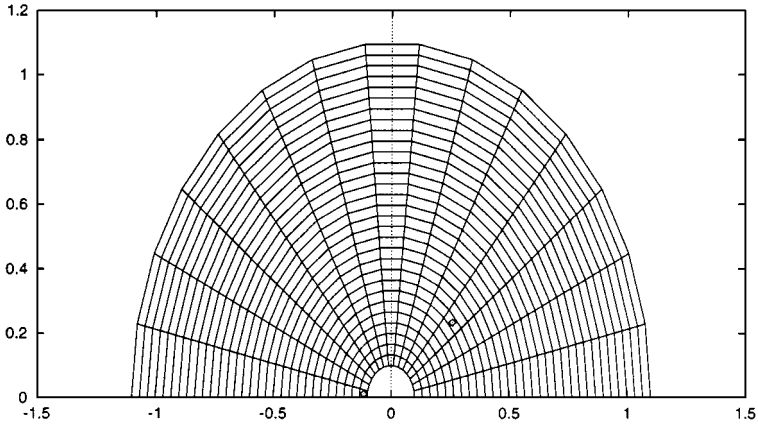

FIG. 10. Grid and observation points $A = (-0.115, 0.0121)$ and $B = (0.259, 0233)$.

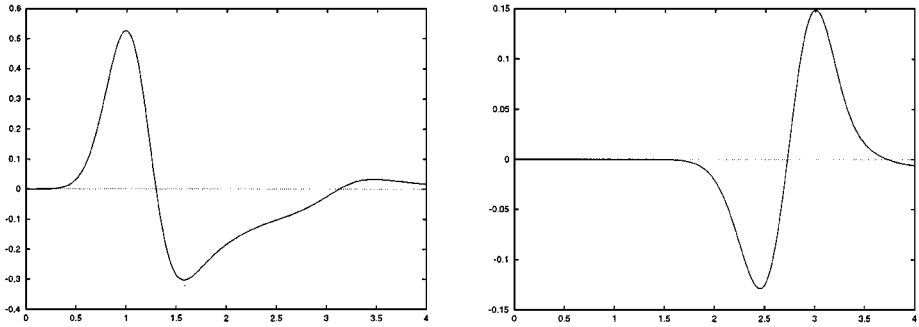

FIG. 11. H_z as a function of time at points $A = (-0.115, 0.0121)$ and $B = (0.259, 0233)$. Time is scaled to ns.

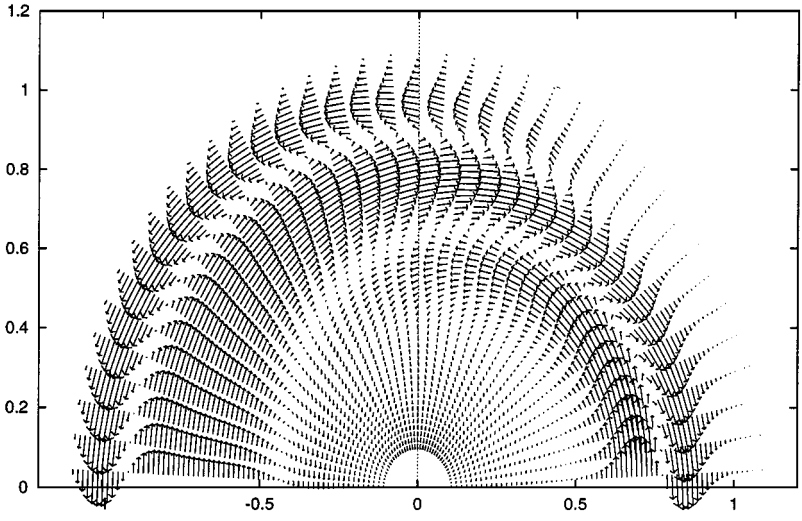

FIG. 12. Electric vector field at $t = 4$ ns.

9. DISCUSSION

We have constructed mimetic FDMs for both the TE and TM modes for 2-D Maxwell's curl equations on nonorthogonal, nonsmooth grids. Because the discrete operators were derived using the discrete vector and tensor analysis developed in [10–13] they satisfy discrete analogs of the main theorems of vector analysis. Because the FDMs satisfy these theorems, they do not have spurious solutions and the "divergence-free" conditions for Maxwell's equations are automatically satisfied.

The tangential components of the electric field and the normal components of magnetic flux used in the FDM are continuous even on discontinuities. This choice guarantees that problems with strongly discontinuous coefficients are treated properly. Furthermore on rectangular grids the method reduces to the analytically correct averaging for discontinuous coefficients. We proved that the implicit mid-point time integration method is conservative and leads to a SPD system of linear equations. On the arbitrary quadrilateral grid we have verified that the convergence rate was between first and second order and demonstrated robustness of the method in numerical examples.

The FDM is formulated in terms of coordinate invariant quantities such as lengths, areas, volumes, and angles. The method can be used in any coordinate system by expressing these quantities in terms of the particular coordinate system. Also, when ϵ, μ, and σ are tensors, the method can be used by changing the form of the $\mathcal{L}$ and $\mathcal{S}$ the same way as it is done for the heat equation with tensor conductivity in [15].

As mentioned in Subsection 5.2, the method can be adapted for impedance boundary conditions and the resulting system of linear equations can also be proved to be SPD (the proof is similar to the one given in [13]).

Although the extension to 3-D hexahedron grids is technically straightforward the details are tedious and depend upon the shape chosen for faces of the 3-D grid cells. A standard way of doing this is to map the hexahedron to reference cube using a tri-linear map. The extension to unstructured grids is also straightforward once the cell, face, and edge are well defined.

The theoretical investigation of the stability and convergence of the FDM described in this paper can be done using an approach similar to the energy method used in [8, 7, 6, 2, 9] for FDMs, or [24, 25] for finite element methods.

We are continuing to develop a discrete version of electromagnetic theory on general grids by extending the discrete theory for uniform rectangular grids [5] based on discrete vector analysis [10–13]. The approach will involve discrete scalar and vector potentials, which can be introduced on the basis of the discrete version of orthogonal decomposition theorems proved in [12].

ACKNOWLEDGMENTS

This work was performed under the auspices of the U.S. Department of Energy (DOE) Contract W-7405-ENG-36 and the DOE/BES (Bureau of Energy Sciences) Program in the Applied Mathematical Sciences Contract KC-07-01-01. The authors acknowledge the reviewers for suggestions; D. Barnes, J. Morel, T. Oliphant, Jr., S. Steinberg for many fruitful discussions; and R. Schuhmann for providing a preprint of his recent work with T. Weiland [34].

REFERENCES

1. A. C. Adam, A. G. Serveniere, J. C. Nedelec, and P. A. Raviart, Study of an implicit scheme for integrating Maxwell's equations, *Comput. Methods Appl. Mech. Eng.* **22**, 327 (1980).

2. N. V. Ardelyan, The convergence of difference schemes for two-dimensional equations of acoustics and Maxwell's equations, *USSR Comput. Math. Math. Phys.* **23**, 93 (1983).
3. A. Bossavit, *Computational Electromagnetism: Variational Formulations, Complementarity, Edge Elements* (Academic Press, San Diego 1998).
4. Z. Cai, J. E. Jones, S. F. McCormick, and T. F. Russell, Control-volume mixed finite element methods, *Comput. Geosci.* **1**, 289 (1997).
5. W. C. Chew, Electromagnetic theory on a lattice, *J. Appl. Phys.* **75**, 4843 (1994).
6. A. A. Denisov, A. V. Koldoba, and Yu. A. Poveshchenko, The convergence to generalized solutions of difference schemes of the reference-operator method for Poisson's equation, *USSR Comput. Math. Math. Phys.* **29**, 32 (1989).
7. M. V. Dmitrieva, A. A. Ivanov, V. F. Tishkin, and A. P. Favorskii, Construction and investigation of support-operators finite-difference schemes for Maxwell equations in cylindrical geometry, preprint, Keldysh Inst. of Appl. Math., USSR Ac. of Sc., 27, 1985. [In Russian]
8. V. Girault, Theory of a finite difference methods on irregular networks, *SIAM J. Numer. Anal.* **11**, 260 (1974).
9. B. Gustafsson, H.-O. Kreiss, and J. Oliger, *Time Dependent Problems and Difference Methods* (Wiley–Interscience, New York, 1995), Chap. 11, p. 445.
10. J. M. Hyman and M. Shashkov, Natural discretizations for the divergence, gradient, and curl on logically rectangular grids, *Int. J. Comput. Math. Appl.* **33**, 81 (1997).
11. J. M. Hyman and M. Shashkov, The adjoint operators for the natural discretizations for the divergence, gradient, and curl on logically rectangular grids, *IMACS J. Appl. Numer. Math.* **25**, 413 (1997).
12. J. M. Hyman and M. Shashkov, The orthogonal decomposition theorems for mimetic finite difference methods, *SIAM J. Numer. Anal.* **36**, 788 (1998).
13. J. M. Hyman and M. Shashkov, The approximation of boundary conditions for mimetic finite difference methods, *Int. J. Comput. Math. Appl.* **36**, 79 (1999).
14. J. M. Hyman and M. Shashkov, *Mimetic Discretizations for Maxwell's Equations and Equations of Magnetic Diffusion*, Report LA-UR-98-1032 (http://cnls.lanl.gov/~shashkov) of Los Alamos National Laboratory, Los Alamos, NM.
15. J. M. Hyman, M. Shashkov, and S. Steinberg, The numerical solution of diffusion problems in strongly heterogeneous non-isotropic materials, *J. Comput. Phys.* **132**, 130 (1997).
16. B. Jiang, J. Wu, and L. A. Pavinelli, The origin of spurious solutions in computational electromagnetics, *J. Comput. Phys.* **125**, 104 (1996).
17. B. Jiang, *The Least-Squares Finite Element Method: Theory and Applications in Computational Fluid Dynamics and Electromagnetics* (Springer-Verlag, New York/Berlin, 1998), p. 371.
18. J. Jin, *The Finite Element Method in Electromagnetics* (Wiley, New York, 1993).
19. T. K. Korshiya, V. F. Tishkin, A. P. Favorskii, and M. J. Shashkov, Flow-variational difference schemes for calculating the diffusion of a magnetic field, *Sov. Phys. Dokl.* **25**, 832 (1980).
20. R. L. Lee and N. K. Madsen, A mixed finite element formulation for Maxwell's equations in the time domain, *J. Comput. Phys.* **88**, 284 (1990).
21. A. R. Maikov, A. G. Sveshnikov, and S. A. Yakunin, Mathematical modeling of a microwave plasma generator, *USSR Comput. Math. Math. Phys.* **25**, 149 (1985).
22. B. J. McCartin and J. F. Dicello, Three dimensional finite difference frequency domain scattering computation using the control region approximation, *IEEE Trans. Magnetics* **25**, 3092 (1989).
23. P. Monk, A comparison of three mixed methods for the time-dependent Maxwell's equations, *SIAM J. Sci. Stat. Comput.* **13**, 1097 (1992).
24. P. Monk, Analysis of finite element method for Maxwell's equations, *SIAM J. Numer. Anal.* **29**, 714 (1992).
25. P. Monk, An analysis of Nedelec's method for the spatial discretization of Maxwell's equations, *J. Comp. Appl. Math.* **47**, 101 (1993).
26. J. E. Morel, R. M. Roberts, and M. Shashkov, A local support-operators diffusion discretization scheme for quadrilateral r-z meshes, *J. Comput. Phys.* **144**, 17 (1998).
27. J. C. Nedelec, Mixed finite elements in R^3, *Numer. Math.* **35**, 315 (1980).

28. R. A. Nicolaides, A discrete vector field theory and some applications, in *Proceedings of IMACS'91—13th IMACS World Congress on Computation and Applied Mathematics, Trinity College, Dublin, Ireland, 1991*, p. 120.
29. R. A. Nicolaides and X. Wu, Covolume solutions of three dimensional DIV-CURL equations, *SIAM J. Numer. Anal.* **34**, 2195 (1997).
30. R. A. Nicolaides and D.-Q. Wang, Convergence analysis of covolume scheme for Maxwell's equations in three dimensions, *Math. Comput.* **67**, 946 (1998).
31. P. A. Raviart and J. M. Thomas, A mixed finite element method for 2-nd order elliptic problems, in *Mathematical Aspects of Finite Element Methods*, edited by I. Galligani and E. Magenes (Springer-Verlag, New York/Berlin, 1977), p. 20.
32. J. R. Reitz, F. J. Milford, and R. W. Christy, *Foundations of Electromagnetic Theory* (Addison–Wesley, Reading, MA) 3rd ed. (1980), Chaps. 16–18.
33. A. A. Samarskii, V. F. Tishkin, A. P. Favorskii, and M. Yu. Shashkov, Operational finite-difference schemes, *Differential Equations* **17**, 854 (1981).
34. R. Schuhmann and T. Weiland, Stability of the FDTD algorithm on nonorthogonal grids related to the spatial interpolation scheme, *IEEE Trans. Magnetics* **34**, 2751 (1998).
35. M. Shashkov, *Conservative Finite-Difference Schemes on General Grids* (CRC Press, Boca Raton, FL, 1995).
36. M. Shashkov, Violation of conservation laws when solving difference equations by the iteration methods, *U.S.S.R. Comput. Math. Math. Phys.* **22**, 131 (1982).
37. M. Shashkov and A. Solov'ov, Finite-difference schemes for solution of heat equation on Dirichlet grid, preprint, All Union Center for Mathematical Modeling, U.S.S.R. Academy of Sciences, 27, 1991. [In Russian]
38. M. Shashkov and S. Steinberg, Support-operator finite-difference algorithms for general elliptic problems, *J. Comput. Phys.* **118**, 131 (1995).
39. M. Shashkov and S. Steinberg, Solving diffusion equations with rough coefficients in rough grids, *J. Comput. Phys.* **129**, 383 (1996).
40. *Finite Elements for Wave Electromagnetics: Methods and Techniques*, edited by P. P. Silvester and G. Pelosi (IEEE Press, New York, 1994).
41. J. A. Shercliff, *A Textbook of Magnetohydrodynamics* (Pergamon, Oxford, 1965), p. 24.
42. A. Taflove, *Computational Electrodynamics: The Finite-Difference Time-Domain Method* (Artech House, Boston, 1995).
43. T. Weiland, Time domain electromagnetic field computation with finite difference methods, *Int. J. Numer. Model.* **9**, 295 (1996).
44. K. S. Yee, Numerical solution of initial boundary value problems involving Maxwell's equations in isotropic media, *IEEE Trans. Antennas Propag.* **14**, 302 (1966).